

Research Articles: Systems/Circuits

Reversible inactivation of ferret auditory cortex impairs spatial and non-spatial hearing

<https://doi.org/10.1523/JNEUROSCI.1426-22.2022>

Cite as: J. Neurosci 2023; 10.1523/JNEUROSCI.1426-22.2022

Received: 20 July 2022

Revised: 16 November 2022

Accepted: 29 November 2022

This Early Release article has been peer-reviewed and accepted, but has not been through the composition and copyediting processes. The final version may differ slightly in style or formatting and will contain links to any extended data.

Alerts: Sign up at www.jneurosci.org/alerts to receive customized email alerts when the fully formatted version of this article is published.

1 **Title:**

2 **Reversible inactivation of ferret auditory cortex impairs spatial and non-**
3 **spatial hearing**

4 **Authors:** Stephen M. Town^{1*}, Katarina C. Poole¹, Katherine C. Wood^{1,2} & Jennifer K. Bizley^{1*}

5 **Author Affiliations:**

6 ¹Ear Institute, University College London, London, UK.

7 ² Department of Otorhinolaryngology: HNS, Department of Neuroscience, University of
8 Pennsylvania, Philadelphia, PA.

9

10 **Corresponding Authors:**

11 Stephen Town (s.town@ucl.ac.uk), UCL Ear Institute, 332 Gray's Inn Road, London, UK

12 Jennifer Bizley (j.bizley@ucl.ac.uk), UCL Ear Institute, 332 Gray's Inn Road, London, UK

13 Abstract

14 A key question in auditory neuroscience is to what extent are brain regions functionally specialized
15 for processing specific sound features such as location and identity. In auditory cortex, correlations
16 between neural activity and sounds support both the specialization of distinct cortical subfields, and
17 encoding of multiple sound features within individual cortical areas. However, few studies have
18 tested the contribution of auditory cortex to hearing in multiple contexts. Here we determined the
19 role of ferret primary auditory cortex in both spatial and non-spatial hearing by reversibly
20 inactivating the middle ectosylvian gyrus during behavior using cooling (n=2 females) or
21 optogenetics (n=1 female). Optogenetic experiments utilized the mDLx promoter to express
22 Channelrhodopsin2 in GABAergic interneurons and we confirmed both viral expression (n=2
23 females) and light-driven suppression of spiking activity in auditory cortex, recorded using
24 Neuropixels under anesthesia (n=465 units from 2 additional untrained female ferrets). Cortical
25 inactivation via cooling or optogenetics impaired vowel discrimination in co-located noise. Ferrets
26 implanted with cooling loops were tested in additional conditions that revealed no deficits for
27 identifying vowels in clean conditions, or when the temporally coincident vowel and noise were
28 spatially separated by 180 degrees. These animals did however show impaired sound localization
29 when inactivating the same auditory cortical region implicated in vowel discrimination in noise. Our
30 results demonstrate that, as a brain region showing mixed selectivity for spatial and non-spatial
31 features of sound, primary auditory cortex contributes to multiple forms of hearing.

32

33 Significance Statement

34 Neurons in primary auditory cortex are often sensitive to the location and identity of sounds. Here
35 we inactivated auditory cortex during spatial and non- spatial listening tasks using cooling, or
36 optogenetics. Auditory cortical inactivation impaired multiple behaviors, demonstrating a role in
37 both the analysis of sound location and identity and confirming a functional contribution of mixed
38 selectivity observed in neural activity. Parallel optogenetic experiments in two additional untrained
39 ferrets linked behavior to physiology by demonstrating that expression of Channelrhodopsin 2
40 permitted rapid light-driven suppression of auditory cortical activity recorded under anesthesia.

41 Introduction

42 A central question in neuroscience is to what extent the brain is functionally organized into
43 specialized units versus distributed networks of interacting regions (Földiák, 2009; Bowers, 2017). In
44 sensory systems, separate cortical fields are thought to process distinct stimulus features such as
45 visual motion, color and identity (Nassi and Callaway, 2009) or sound location and identity
46 (Rauschecker and Scott, 2009).

47 Primary auditory cortex plays a critical role in many aspects of hearing. Neurons in this area show
48 tuning to multiple features of sounds such as location and level (Brugge et al., 1996; Zhang et al.,
49 2004), location and identity (Amaro et al., 2021) or vowel timbre, pitch and voicing (Bizley et al.,
50 2009; Town et al., 2018). This sensitivity to multiple features can give rise to complex
51 spectrotemporal tuning (Atencio et al., 2008; Harper et al., 2016) that can also be modulated by
52 ongoing behavior (Fritz et al., 2003; David et al., 2012).

53 The mixed selectivity observed in responses of auditory cortical neurons is matched by a diverse
54 range of behavioral deficits following auditory cortical lesions or inactivation (Slonina et al., 2022).
55 Affected behaviors include discrimination of natural sounds such as vocalizations (Heffner and
56 Heffner, 1986; Harrington et al., 2001), as well as sound modulation (Ohl et al., 1999; Ceballo et al.,
57 2019) and sound localization (Heffner and Heffner, 1986; Malhotra et al., 2008). Most cortical
58 inactivation studies focus on performance in a single task, or on a small range of related behaviors
59 and thus our inferences on common functions must draw on data from different subjects, species
60 and techniques.

61 Ideally, we would complement such inferences with direct comparisons of the effects of inactivation
62 on distinct tasks performed by the same subjects and using the same methods of perturbation. Tests
63 of distinct behaviors during auditory cortical inactivation are rare, but have yielded valuable insight
64 into the functional specialization of non-primary auditory cortex (Adriani et al., 2003; Lomber and
65 Malhotra, 2008; Ahveninen et al., 2013).

66 Here, we define distinct behaviors as those requiring subjects to act on the basis of orthogonal
67 stimulus features, where orthogonality indicates that one feature can be varied while another
68 remains constant (e.g. Flesch et al., 2018). The sparsity of inactivation data across distinct behaviors
69 reflects the technical limitations on suppressing neural activity in humans and the difficulty in
70 training individual animals to perform multiple tasks with contrasting demands.

71 We leveraged ferrets' capacity to learn multiple psychoacoustic tasks to test the role of auditory
72 cortex in distinct behaviors involving vowel discrimination in multiple contexts (clean conditions, or
73 with co-located or spatially separated noise) and approach-to-target sound localization. During
74 testing, we reversibly inactivated a large portion of primary auditory cortex by cooling the mid-to-
75 low frequency area of the middle ectosylvian gyrus (MEG). Inactivation produced a pattern of
76 deficits that confirms a common role for this brain region in both spatial and non-spatial hearing.
77 Further experiments with optogenetics confirmed the role for MEG in vowel discrimination in noise
78 and demonstrated the efficacy of light-driven suppression of sound evoked responses in ferret
79 auditory cortex.

80 **Methods**

81 **Animals**

82 Subjects were ten pigmented ferrets (*Mustela putorius*, female, between 0.5 and 5 years old).
83 Animals were maintained in groups of two or more ferrets in enriched housing conditions, with
84 regular otoscopic examinations to ensure the cleanliness and health of ears.

85 Seven animals were trained in behavioral tasks in which access to water was regulated (**Table 1**).
86 During water regulation, each ferret was water-restricted prior to testing and received a minimum of
87 60ml/kg of water per day, either during task performance or supplemented as a wet mash made
88 from water and ground high-protein pellets. Subjects were tested in morning and afternoon sessions
89 on each day for up to five days in a week, while their weight and water consumption was measured
90 throughout the experiment.

91 All experimental procedures were approved by local ethical review committees (Animal Welfare and
92 Ethical Review Board) at University College London and The Royal Veterinary College, University of
93 London and performed under license from the UK Home Office (Project License 70/7267) and in
94 accordance with the Animals (Scientific Procedures) Act 1986.

95 **Stimuli**

96 Vowel discrimination

97 Vowels were synthesized in MATLAB (MathWorks, USA) using an algorithm adapted from Malcolm
98 Slaney's Auditory Toolbox (<https://engineering.purdue.edu/~malcolm/interval/1998-010/>) that
99 simulates vowels by passing a click train through a biquad filter with appropriate numerators such
100 that formants are introduced in parallel. In the current study, four formants (F1-4) were modeled:
101 /u/ (F1-4: 460, 1105, 2857, 4205 Hz), /ε/ (730, 2058, 2857, 4205 Hz), /a/ (936, 1551, 2975, 4263 Hz)
102 and /i/ (437, 2761, 2975, 4263 Hz). Each ferret was were only trained to discriminate between a pair
103 of vowels: either /ε/ and /u/ (F1201, F1203, F1217, F1509 and F1706), or /a/ and /i/ (F1216 and
104 F1311). All vowels were generated with a 200 Hz fundamental frequency.

105 Vowels were presented in clean conditions as two repeated tokens, each of 250 ms duration and of
106 the same identity, separated with a silent interval of 250 ms (**Fig. 1A**). Here, two vowel tokens were
107 used for consistency with previous work (Bizley et al., 2013a; Town et al., 2015). Sounds were
108 presented through loudspeakers (Visaton FRS 8) positioned on the left and right sides of the head at
109 equal distance and approximate head height. These speakers produced a smooth response (± 2 dB)
110 from 200 to 20000 Hz, with a 20 dB drop-off from 200 to 20 Hz when measured in an anechoic
111 environment using a microphone positioned at a height and distance equivalent to that of the
112 ferrets in the testing chamber. All vowel sounds were passed through an inverse filter generated
113 from calibration of speakers to Golay codes (Zhou et al., 1992). Clean conditions were defined as the
114 background sound level measured within the sound-attenuating chamber in which the task was
115 performed in the absence of stimulus presentation (22 dB SPL).

116 Vowels were also presented with additive broadband noise fixed at 70 dB SPL generated afresh on
117 each trial. The noise was timed to ramp on at the onset of the first vowel token and ramp off at the
118 end of the second vowel token, and thus had a total duration of 750 ms (i.e. that was equal to the

119 two vowel tokens, plus the intervening silent interval). Onsets of both vowels and noise were ramped
120 using a 5 ms cosine function. During initial experiments on vowel discrimination in noise, vowels and
121 noise were played from both left and right speakers (**Fig. 1A**); however when investigating spatial
122 release from energetic masking, vowels were presented from either left or right speaker but not
123 both. Noise was also presented from one speaker and thus the noise levels in such experiments were
124 67 dB SPL; noise was presented either from the same speaker as vowels, the opposite speaker or not
125 at all (**Fig. 1B**).

126 Sound localization

127 Auditory stimuli were broadband noise bursts of differing durations (F1509: 700 ms; F1311: 250 ms
128 or 100 ms) cosine ramped with 5-ms duration at the onset and offset and low-pass filtered below 22
129 kHz (finite impulse response filter <22 kHz, 70 dB attenuation at 22.2 kHz). Noise bursts were
130 generated afresh on each trial in MATLAB at a sampling frequency of 48828.125 Hz and presented
131 from one of seven speakers (Visaton FRS SC 5.9) positioned at 30° intervals (**Fig. 1C**). Note that one
132 ferret (F1509) was not tested with sounds from the central speaker (0°). Across trials, stimuli were
133 presented at one of three pseudo-randomly selected intensities (57, 61.5 and 66 dB SPL).

134 Speakers were calibrated to produce a flat response from 200 Hz to 25 kHz using Golay codes,
135 presented in an anechoic environment, to construct inverse filters (Zhou et al., 1992). All the
136 speakers were matched for level using a microphone positioned upright at the level of the ferret's
137 head in the center of the semi-circle. Calibrations were performed with a condenser microphone
138 (Model 4191, Brüel and Kjær) and/or a Brüel and Kjær 3110–003 measuring amplifier.

139 **Task design**

140 Behavioral tasks, data acquisition, and stimulus generation were all automated using custom
141 software running on personal computers, which communicated with TDT real-time signal processors
142 (Vowel discrimination: RZ6, Sound localization: RX8).

143 Vowel discrimination

144 Ferrets were trained to discriminate between synthetic vowel sounds by reporting at a left response
145 port if one type of vowel (e.g. /u/) was presented, or reporting at a right response port if a second
146 type of vowel (e.g. /ε/) was presented. For each animal, the association between vowel identity and
147 response location was maintained across all experiments with vowel sounds.

148 Experiments were performed within a custom-built double-walled sound attenuating chamber (IAC
149 Acoustics Ltd.) lined with acoustic foam. The chamber contained a wire-frame pet-cage with three
150 response ports housing infra-red sensors that detected the ferret's presence. On each trial, the
151 ferret was required to approach the center port and hold head position for a variable period
152 (between 0 and 500 ms) before stimulus presentation. Animals were required to maintain contact
153 with the center port until 250 ms after the presentation of the first token, at which point they could
154 respond at left or right response ports. Correct responses were rewarded with water while incorrect
155 responses led to a brief time-out (between 3 and 8 s) indicated by presentation of a 100 ms
156 broadband noise burst and in which the center port was disabled so that animals could not initiate a
157 new trial. Following a time-out, the animal was presented with a correction trial in which the same
158 stimulus and trial parameters (e.g. hold time) were used. To suppress any bias the animal might have
159 to respond at a particular port, we continued to present timeouts and correction trials until a correct

160 response was made. Once a correct response was made on correction trials, a new vowel sound and
161 trial parameters were selected for the next trial. To encourage animals to maintain a steady head
162 position at the center port during sound presentation, a water reward was also given at trial onset
163 on a small proportion (10%) of randomly chosen trials.

164 Sound localization

165 Ferrets were trained and tested in a second behavioral chamber that consisted of a custom-built D-
166 shaped box surrounded by an array of seven speakers at 30° intervals. Each speaker had a response
167 port located in front (8.5 cm in front of the speaker; 15.5 cm from the center of the box) at which
168 animals could report sound location and obtain water rewards. A further port was also placed at the
169 center of the arena to initiate stimulus presentation. This port was offset from the center by 3 cm to
170 ensure the animal's head was aligned at the center of the speaker ring, with the interaural axis in
171 line with the -90° and +90° speakers. The distance between the head and speakers during sound
172 presentation was 24 cm. Outside the training box, an LED (15 cm from the floor) was used to
173 indicate trial availability. The test arena was housed in a custom built sound attenuating chamber
174 (90 cm high x 90 cm wide x 75 cm deep, Zephyr Products Ltd, UK) lined with 45 mm acoustic foam.

175 **Behavioral training**

176 Vowel discrimination

177 Subjects were trained to discriminate a pair of vowels through a series of stages of increasing
178 difficulty. When first introduced to the training apparatus, animals were rewarded with water if they
179 visited any port. Once subjects had associated the ports with water, a contingency was introduced in
180 which the subject was required to hold the head at the central port for a short time (501–1001 ms)
181 before receiving a reward. The central port activation initiated a trial period in which a nose-poke at
182 either peripheral port was rewarded.

183 Following acquisition of the basic task structure (typically two to three sessions), sounds were
184 introduced. On each trial, two repeats of a single vowel sound (each 250 ms in duration with a 250
185 ms interval) were played after the animal first contacted the port with a variable delay (between 0
186 and 500 ms). A trial was initiated if the subject's head remained at the port for the required hold
187 time, plus an additional 500 ms in which the first token of the sound and subsequent interval were
188 played. Following trial initiation, vowel sounds were looped (i.e. played repeatedly) until the ferret
189 completed the trial by visiting the "correct" peripheral port to receive a reward. Nose-pokes at the
190 "incorrect" peripheral port were not rewarded or punished at this stage and incorrect responses did
191 not terminate trials. If the animal failed to visit the correct port within a specified period after
192 initiating a trial (between 25 and 60 s), that trial was aborted and the animal could begin the next
193 trial.

194 Once animals were completing trials frequently, the consequences of incorrect responses were
195 altered so that incorrect responses terminated the current trial. Subjects were then required to
196 return to the center port to initiate a correction trial in which the same stimulus was presented.
197 Correction trials were included to prevent animals from biasing their responses to only one port and
198 were repeated until the animal made a correct response. After a minimum of two sessions in which
199 errors terminated trials, a time-out (between 5 and 15 s) punishment was added to incorrect

200 responses. Time-outs were signaled by a burst of broadband noise (100 ms), and the center port was
201 disabled for the duration of the time out, preventing initiation of further trials.

202 Once subjects could discriminate repeated sounds on consecutive sessions with a performance of
203 80%, looping of sounds was removed so that subjects were presented with only two repeated vowel
204 sounds during the initiation of the trial at the center port. When ferrets correctly identified 80% of
205 vowels in two consecutive sessions, the animal was considered to be ready for testing in noise. Note
206 that beyond experience through testing, ferrets did not receive specific training to discriminate
207 vowels in noise.

208 Sound localization

209 In contrast to vowel discrimination, training in sound localization took place after animals were
210 implanted with cooling loops, and following completion of all testing in vowel discrimination. Ferrets
211 (F1311 and F1509) were first trained to hold at the port in the center of the localization arena to
212 initiate presentation of a series of repeating 1000 ms noise bursts (500 ms interval) from one
213 speaker. The animal was allowed to leave the central port after the first burst, after which the
214 stimulus repeated until a correct response was made at the peripheral port nearest the presenting
215 speaker. Responses at other ports had no effect at this stage, but premature departures from the
216 center triggered a short (1 sec) timeout.

217 Once ferrets were accustomed to the task (identified by regularly returning to the start port after
218 receiving water from target locations), error detection was introduced so that trials were terminated
219 when animals reported at the wrong peripheral port. The ferret was then required to initiate a new
220 trial, on which the same stimulus was presented (correction trial) until a correct response was made.
221 Time-outs were then introduced for incorrect responses and were increased from 1 to between 5
222 and 7 seconds. During this training phase, we also increased the hold time required at the central
223 port before stimulus presentation, initially up to 500 ms during training and then 1000 ms during
224 testing.

225 Once ferrets reached $\geq 60\%$ correct, the stimulus was reduced to a single noise burst and
226 subsequently the stimulus duration was reduced. Ferrets were ready for testing at these durations
227 once their performance stabilized (approximately 3 to 4 weeks); for one ferret (F1311) we could
228 reduce sound duration to between 250 and 100 ms with stable performance, however time
229 constraints on the lifetime of the cooling implant required that we use a longer duration (700 ms) for
230 the second animal (F1509). In all cases, animals were required to hold head position at the central
231 port for the full duration of the sound and thus could not make head movements during stimulus
232 presentation.

233 **Cortical inactivation using cooling**

234 Loop implantation

235 Cortical inactivation experiments were performed using an approach developed by Wood et al.
236 (2017): Two ferrets (F1311 & F1509) were successfully implanted with cooling loops made from 23
237 gauge stainless steel tubing bent to form a loop shape approximately the size of primary auditory
238 cortex. (A third ferret, F1216, was also implanted but the loops were persistently blocked and thus
239 non-functional). At the base of the loop, a micro-thermocouple made from twisting together PFA
240 insulated copper (30 AWG; 0.254 mm) and constantan wire (Omega Engineering Limited, UK), was

241 soldered and secured with araldite. Thermocouple wires were soldered to a miniature thermocouple
242 connector (RS components Ltd, UK) and secured with epoxy resin prior to implantation.

243 Loops were surgically implanted over the middle ectosylvian gyrus, specifically targeting the mid-to-
244 low frequency regions of primary auditory cortex (A1 and Anterior Auditory Field, AAF) that border
245 the non-primary fields of the posterior Ectosylvian gyrus (**Fig. 2A**). Loops targeted this region as it is
246 known to contain neurons sensitive to both sound timbre and location (Bizley et al., 2009; Town et
247 al., 2018). Consistent with previous studies (Wood et al., 2017), we did not map the boundaries of
248 auditory cortical subfields prior to loop placement. Cortical mapping may damage brain tissue,
249 potentially triggering compensatory mechanisms that might mask a role in task performance.
250 Placement of cooling loops was therefore based on our extensive experience targeting this area for
251 electrode placements using anatomical landmarks (Bizley et al., 2009, 2013b; Town et al., 2018).

252 Surgery was performed in sterile conditions under general anesthesia, induced by a single
253 intramuscular injection of diazepam (0.4 ml/kg, 5 mg/ml; Hameln) and ketamine (Ketaset; 0.25
254 ml/kg, 100 mg/ml; Fort Dodge Animal Health, Kent, UK). Animals were intubated and ventilated, and
255 anesthesia was then maintained with between 1 and 3% isoflurane in oxygen throughout the
256 surgery. Animals were provided with subcutaneous injections of atropine (0.09 ml/kg, 600 µl/ml)
257 and dexamethasone (0.25 ml/kg), as well as surgical saline intravenously, while vital signs (body
258 temperature, end-tidal CO₂, Oxygen saturation and electrocardiogram) were monitored throughout
259 surgery.

260 General anesthesia was supplemented with local analgesics (Marcaine, 2 mg/kg, AstraZeneca)
261 injected at the point of midline incision. Under anesthesia, the temporal muscle overlying the skull
262 was retracted and largely removed, and a craniotomy was made over the ectosylvian gyrus. The dura
263 over the gyrus was then opened to allow placement of the cooling loop on the surface of the brain.
264 The loop was shaped during surgery to best fit the curvature of the cortical surface prior to
265 placement, and was then embedded within silicone elastomer (Kwik-Sil, World Precision
266 Instruments) around the craniotomy, and dental cement (Palacos R+G, Heraeus) on the head. Bone
267 screws (stainless steel, 19010-100, Interfocus) were also placed along the midline and rear of the
268 skull (two per hemisphere) to anchor the implant. Implant anchorage was also facilitated by cleaning
269 the skull with citric acid (0.1 g in 10 ml distilled water) and application of dental adhesive (Supra-
270 Bond C&B, Sun Medical). Some skin was then removed in order to close the remaining muscle and
271 skin smoothly around the edges of the implant.

272 Pre-operative, peri-operative and post-operative analgesia and anti-inflammatory drugs were
273 provided to animals under veterinary advice. Animals were allowed to recover for at least one
274 month before resuming behavioral testing and beginning cortical inactivation experiments.

275 Cooling during behavior

276 To reduce the temperature of the cortical tissue surrounding the loop, cooled ethanol (100%) was
277 passed through the tube using an FMI QV drive pump (Fluid Metering, Inc., NY, USA) controlled by a
278 variable speed controller (V300, Fluid Metering, Inc., NY, USA). Ethanol was carried to and from the
279 loop on the animal's head via FEP and PTFE tubing (Adtech Polymer Engineering Ltd, UK) insulated
280 with silicon tubing and, where necessary, bridged using two-way connectors (Diba Fluid Intelligence,
281 Cambridge, UK). Ethanol was cooled by passage through a 1 meter coil of PTFE tubing held within a

282 Dewar flask (Nalgene, NY, USA) containing dry ice and ethanol. After passing through the loop to
283 cool the brain, ethanol was returned to a reservoir that was open to atmospheric pressure.

284 For a cooling session, the apparatus was first 'pre-cooled' before connecting an animal by pumping
285 ethanol through spare cooling loops (i.e. loops that were not implanted in an animal) until loop
286 temperatures fell below 0°C. The animal was then connected to the system, using the implanted
287 thermocouples to monitor loop temperature at the cortical surface (**Fig. 2B**). The temperature was
288 monitored online using a wireless transfer system (UWTC-1, Omega Engineering Ltd., UK) or wired
289 thermometer, and pump flow rates adjusted to control loop temperature. Loops over both left and
290 right auditory cortex were connected during bilateral cooling (all tasks), whereas only the left or
291 right loop was connected during unilateral cooling (sound localization only).

292 For F1311, the animal was connected to the system and cooling began before the behavioral
293 session, with the subject held by the experimenter and rewarded with animal treats (Nutriplus gel,
294 Virbac, UK) while cooling pumps were turned on and loop temperatures reduced over five to ten
295 minutes. When loop temperatures reached $\leq 12^\circ\text{C}$, the animal was placed in the behavioral arena
296 and testing began. In contrast, F1509 would not perform tasks after being rewarded by the
297 experimenter and so behavioral sessions were started and cortical temperature slowly reduced
298 during task performance. Trials performed before the loops reached $\leq 20^\circ\text{C}$ were excluded from
299 analysis. Across animals, we targeted temperatures between 8 and 20°C (**Fig. 2B**) that should
300 suppress spiking activity within the immediate vicinity of the loop without spreading beyond the
301 ectosylvian gyrus (Lomber et al., 1999; Coomber et al., 2011; Wood et al., 2017).

302 For both animals, cooling took place while the animals were free to move without interaction with
303 the experimenter and within the same apparatus used for previous behavioral testing. The
304 behavioral tasks during cooling were unchanged from those already described; i.e. the same ranges
305 of sound levels were used, correction trials were included and the same reward contingencies were
306 used. For each trial in the task, the time of stimulus onset was recorded and cross-referenced with
307 temperature records so that any trials in which cortical temperature was above threshold during a
308 cooling session could be removed from the analysis. During control testing, animals were connected
309 to the cooling system using the same thermocouple sensors, but cooling loops were not connected
310 to FEP tubing in order to avoid blockages and maximize the functional lifespan of loops.

311 **Data analysis: Behavior**

312 All analyses excluded responses on correction trials, or trials where ferrets failed to respond within
313 the required time (60 s). For all tests of vowel discrimination, we also required a minimum number
314 of trials ($n=10$) and sessions ($n=3$) in both cooled and control conditions to include a sound level or
315 SNR value in the analysis. Note that the requirement for a minimum number of trials introduced
316 slight differences in the range of levels or SNRs tested between vowel discrimination experiments
317 using vowel presentation both from left and right speakers and spatial release from energetic
318 masking.

319 Temperature measurements were obtained on each trial for loops over left and right auditory
320 cortex, and the animal was considered to be cooled if the average loop temperature was $\leq 20^\circ\text{C}$
321 (bilateral cooling). In unilateral cooling, cooling was considered to be achieved if the relevant loop

322 was $\leq 20^{\circ}\text{C}$. The threshold for cooling was based on previous work demonstrating the suppression of
323 neural activity below this temperature (Jasper et al., 1970; Lomber et al., 1999).

324 Statistical analysis of effects of stimulus manipulation (e.g. presence of noise) and cooling used
325 generalized linear mixed models (GLMMs) fitted using *lme4* (Bates et al., 2015) in R (version 4.2.1).
326 The details of each model are outlined alongside the relevant results; however, in general, analysis
327 of behavioral performance (correct vs. incorrect responses) was based on logistic regression in which
328 the GLMM used binomial distribution and logit link function settings. For each model, we used ferret
329 as a random factor and reported the magnitude of coefficients (β) of fixed effects of interest (e.g.
330 effect of cooling) and probability (p) that the coefficient was drawn from a distribution centered
331 about zero. To check model fit, we used the *DHARMA* package to assess the randomized quantile
332 residuals (Dunn and Smyth, 1996) and reported both the marginal and conditional R^2 values
333 (Nakagawa and Schielzeth, 2013).

334 Vowel Discrimination

335 To analyze the effects of cooling, we compared behavioral performance of each animal across
336 multiple sessions: The effects of cooling were measured on paired testing sessions performed on the
337 same day (F1509) or unpaired sessions collected over the same time period (F1311). For F1509, we
338 excluded trials when the animal was tested with sound levels below 50 dB SPL, for which no other
339 subject was tested.

340 To summarize performance of each subject in a particular stimulus condition (clean conditions, co-
341 located noise etc.), we randomly resampled (bootstrapped) data with equal numbers of each vowel
342 and sound level or SNR (when showing data across level or SNR). Bootstrapping was performed 10^3
343 times, with samples drawn with replacement on each iteration. For each bootstrap iteration, the
344 number of samples drawn for each sound level or SNR was defined by taking the median of the
345 number of trials sampled at each level or SNR. (For example, if we originally collected 10, 20 and 30
346 trials at 50, 60 and 70 dB SPL, we randomly drew 20 trials with replacement for each sound level).
347 Where vowels varied in sound location, we also resampled with equal numbers of trials with vowels
348 from left and right speakers.

349 Sound Localization

350 Performance localizing sounds was analyzed using the percentage of trials on which animals
351 correctly reported the target stimulus position. For F1311, we included responses to sounds of 100
352 ms and 250 ms duration, and sampled a random subset of data to ensure equal numbers of trials
353 with each sound duration were included for each cooling condition. For each animal, we considered
354 control data from all sessions after training was complete, and all trials obtained during cooling.
355 When bootstrap resampling, we randomly drew equal numbers of trials when sounds were
356 presented at each location (F1311: 69 trials at each of seven locations; F1509: 27 trials at each of six
357 locations).

358 **Optogenetics**

359 Injections in Auditory Cortex

360 Four ferrets (F1706, F1801, F1807 and F1814; Table 1) were injected bilaterally in auditory cortex
361 with an Adeno-associated Virus (AAV) to induce expression of Channelrhodopsin 2 (ChR2) in
362 GABAergic interneurons using the mDlx promoter (AAV2.mDlx.ChR2-mCherry-Fishell3.WPRE.SV40,

363 Addgene83898, UPenn Vector Core)(Dimidschstein et al., 2016). For each auditory cortex (i.e. left
364 and right), injections were placed at two sites in the same area of MEG in which cooling loops were
365 placed, under general anesthesia using the same sterile surgical protocol as described above. Within
366 each site, injections were made at two depths (500 and 800 μm below the cortical surface) so that a
367 total of four injections were made per hemisphere, with 1 μl injected each time.

368 Optogenetic testing during behavior (F1706)

369 Following viral delivery, we implanted an optrode (Neuronexus, Ann Arbor, MI, USA) in each
370 auditory cortex to deliver light in F1706. During testing, light was delivered from a 463 nm DPSS laser
371 (Shanghai Laser & Optics Century Ltd. China) with a steady-state power of 40 mW, measured at fiber
372 termination before the optrode using an S140C integrating sphere photodiode sensor (ThorLabs,
373 Germany). Although the optrode implanted included recording sites for monitoring neural activity
374 during testing, we were unable to eliminate grounding issues that made recordings from this animal
375 unusable and we therefore elected to train the animal in the vowel discrimination task and look for
376 behavioral effects of silencing auditory cortex. The optrode was housed within an opaque plastic
377 tower (25 mm tall) embedded in dental cement.

378 Retraining and testing of this animal after viral injection and optrode implantation was delayed due
379 to the Covid-19 pandemic and behavioral testing took place 20 months after injection. At this point,
380 we were only able to test the effect of light delivery on vowel discrimination in noise and a
381 subsequent failure in the implant precluded testing of vowel discrimination in clean conditions, or
382 with stimuli used to study spatial release from energetic masking or sound localization. The implant
383 failure also prevented us from perfusing the brain of this animal in order to detect viral expression
384 (although see below for successful confirmation of viral expression in other animals).

385 All data during vowel discrimination in noise was collected when the animal was attached to the
386 optical fiber system, with opaque black tape used to secure the attachment and ensure that laser
387 light was not visible to the ferret. In behavioral testing, light was delivered on 50% of test trials (with
388 the exception of the first test session in which the laser was presented on all test trials); however, all
389 correction trials took place without light delivery. On each trial that light was presented, we used
390 short pulses (10 ms duration, presented at 10 Hz) that began 100 ms before sound onset, and
391 continued until 100 ms after sound offset.

392 Data analysis for performance discriminating vowels in noise followed the same procedure as for
393 analysis of behavior in animals with cooling. However, optogenetics provided more refined temporal
394 control than cooling, allowing us to compare performance on trials within the same test session,
395 with and without light delivery.

396 Optogenetic suppression of cortical activity (F1801 and F1807)

397 Photostimulation in visual cortex of ferrets expressing ChR2 in GABAergic interneurons suppresses
398 cortical activity (Wilson et al., 2018). To determine if stimulation of ChR2 in GABAergic neurons was
399 also sufficient to suppress sound-driven responses in auditory cortex, we recorded the activity of
400 auditory cortical neurons while presenting stimuli with and without laser stimulation to ferrets
401 under anesthesia.

402 Anesthesia was induced by a single dose of ketamine (Ketaset; 5 mg/kg/h; Fort Dodge Animal
403 Health) and medetomidine (Domitor; 0.022 mg/ kg/h; Pfizer). The left radial vein was cannulated

404 and anesthesia was maintained throughout the experiment by continuous infusion (ketamine: 5
405 mg/kg/hr; medetomidine: 0.022 mg/kg/hr; atropine sulfate: 0.06 mg/kg/hr and dexamethasone: 0.5
406 mg/kg/hr in Hartmann's solution with 5% glucose). The ferret was intubated, placed on a ventilator
407 (Harvard Model 683 small animal ventilator; Harvard Apparatus) and supplemented with oxygen.
408 Body temperature (38°C), electrocardiogram and end-tidal CO₂ were monitored throughout the
409 experiment (~48 hours).

410 Animals were then placed in a stereotaxic frame and the site of viral injection over both left and
411 right auditory cortex was exposed. A metal bar was attached to the midline of the skull, holding the
412 head without further need of a stereotaxic frame. The animal was then transferred to a small table
413 in a soundproof chamber (Industrial Acoustics, Winchester, UK) for stimulus presentation and neural
414 recording. During recordings, the craniotomy was covered with 3% agar, replaced at regular
415 intervals.

416 Neural activity was recorded in SpikeGLX (v 3.0., billkarsh.github.io/SpikeGLX) using Neuropixels
417 Probes (IMEC, v1.0) inserted orthogonal to the cortical surface, and connected via headstages to an
418 IMEC PXIe data acquisition module within PCI eXtensions for Instrumentation (PXI) hardware (PXIe-
419 1071 chassis and PXI-6132 I/O module, National Instruments) that sampled neural signals at 30 kHz.
420 Candidate action potentials were then extracted and sorted in Kilosort (v3.0.,
421 github.com/MouseLand/Kilosort), and manually curated to identify single (n = 174) or multi-unit (n =
422 291) activity. Spike clusters were merged based on assessment of waveform similarity and classed as
423 a single unit using waveform size, consistency and inter-spike interval distribution (all single units
424 had ≤2% of spikes within 2ms). Neural spikes had biphasic waveforms that were notably different
425 from positive-going monophasic waveforms containing sharp peaks that were interpreted as laser
426 artifacts and discarded from the analysis.

427 During recording, we presented broadband noise bursts of varying levels (40 to 70 dB SPL) and
428 durations (50, 100 and 250 ms), either alone or with laser on. Stimuli were repeated 20 times, with a
429 pseudo-random interval (0.5 to 0.7 seconds) between trials. Laser stimulation was provided by the
430 same 463 nm DPSS laser used in behavioral experiments with F1706, attached to a custom made
431 optic-fiber (1.5 mm diameter, Thorlabs FP1500URT) that was designed to maximize the area over
432 which light was delivered, and could provide up to 300 mW at the fiber tip. Here, we report effects
433 of pulsed light, delivered with a target power of 50 mW and frequency of 1 or 10 Hz. Pulses had a
434 square-wave design with 50% duty cycle, beginning 100 ms before sound onset and ending 100 ms
435 after sound offset. In addition to laser testing with sound presentation, we also tested the effect of
436 the laser on spontaneous activity without sound. The effects of laser light delivery were measured at
437 several sites over auditory cortex by placing the optic fiber and Neuropixel probe in various
438 configurations over MEG and close to the viral injection sites of auditory cortex in each animal. Due
439 to the Covid-19 pandemic, recordings were delayed until 21 months (F1801) and 18 months (F1807)
440 after viral injection.

441 After recordings were completed, each animal was transcardially perfused with 0.9% saline and 4%
442 paraformaldehyde (PFA) under anesthesia. The brain was then removed for storage in PFA, before
443 sinking in 30% sucrose for 5 days prior to cryosectioning. Due to unavailability of a functioning
444 cryostat (also delayed by the pandemic), brains were stored in PFA for six months, potentially
445 limiting the quality of fluorescent signals. Coronal sections (50 μm) were taken through the full

446 extent of the ectosylvian gyrus in order to confirm viral expression via visualization of mCherry. To
447 better judge the quality of viral expression on a shorter timescale, we also transcardially perfused a
448 further animal (F1814) within 12 weeks of viral injection, sectioned it immediately and measured
449 mCherry and cell body (DAPI) labeling. Slices were imaged using a Zeiss Axio Imager 2.0 and Zeiss
450 Confocal, and processed on Zen Blue.

451 **Data analysis: Optogenetic modulation of neural activity**

452 To contrast the effects of laser light delivery on sound-driven activity, we first calculated the mean
453 firing rate of each unit during auditory evoked activity, taking a window from sound onset to sound
454 offset (50, 100 or 250 ms in length). For each unit, we compared the mean firing rate during this
455 window calculated over all conditions in which the laser was present with the mean firing rate when
456 the laser was absent (change in firing rate = laser OFF - laser ON). To contrast the effects of laser
457 light delivery on spontaneous activity of each unit, we performed the same calculation on mean
458 firing rates during the 100ms window before sound onset, on trials with and without the laser.

459 Inspection of neural activity with, and without laser suggested that light delivery had distinct effects
460 on subgroups of neurons. To test if units could be distinguished by their modulation to laser delivery
461 and to determine the number of separable groups of units using an unsupervised approach, we
462 applied K-means clustering to the firing rates of each unit with and without laser. Clustering was
463 based on the cosine distance between units (rather than Euclidean distance) in order to isolate the
464 change in spike rate with laser stimulation across units with widely varying baseline firing rates. We
465 identified the appropriate number of clusters within the data by comparing the sum of point-to-
466 centroid distances for K = 1 to 10 and finding the knee-point using vector bisection (Dmitry Kaplan
467 2022. Knee Point, MATLAB Central File Exchange.
468 www.mathworks.com/matlabcentral/fileexchange/35094-knee-point).

469 To map the extent of sound-evoked activity across the length of the probe, we compared mean
470 spike rates during sound presentation and a time window preceding sound onset of matched
471 duration (Wilcoxon signed-rank test). This analysis was performed on each unit to each sound
472 duration by sound level condition, with Bonferroni correction for multiple comparisons. Units that
473 showed a significant response in any of the conditions were classed as an auditory evoked unit ($n =$
474 72). We then contrasted the effects of laser light delivery on the firing rates of units recorded at
475 different cortical depths during sound presentation, where depth refers to the distance on the probe
476 from the most superficial channel on which spiking activity was observed.

477 We also investigated the temporal dynamics of the optogenetic stimulation to control for heating
478 effects from laser delivery (Owen et al., 2019). To identify the latency at which light delivery induced
479 a significant change in firing, we performed nonparametric cluster statistical analysis, which controls
480 for multiple comparisons that would occur from calculating a test-statistic over each timepoint, by
481 calculating a test-statistic from clusters of adjacent time samples of the PSTH in which firing rate
482 with laser was greater than without laser (or vice versa)(Maris and Oostenveld, 2007). This statistic
483 was calculated during the 100 ms after laser onset for each condition and the minimum time bin
484 labeled as significant by the cluster statistic was averaged across conditions to calculate the latency
485 for each unit.

486 **Results**

487 **Optogenetic inactivation of sound-driven responses in auditory cortex**

488 We used an AAV vector with an mDlx promoter to target expression of ChR2 to GABAergic
489 interneurons in ferret auditory cortex. Post-mortem histology confirmed viral expression in two of
490 three animals perfused (F1807 and F1814, but not F1801, in whom terminal recordings had severely
491 compromised brain quality). Widefield imaging demonstrated viral expression in MEG, with labeled
492 cells observed up to between 1 and 2 mm from injection sites (**Fig. 3A**). Confocal imaging revealed
493 colocalization of mCherry with cell bodies (labeled by DAPI), with the opsin localized around the cell
494 body (F1814).

495 We then examined the electrophysiological efficacy of cortical inactivation through optogenetics
496 using Neuropixels probes to record the activity of 465 units (n = 174 single units, 291 multi-units) in
497 auditory cortex under ketamine-medetomidine anesthesia. Multiple optic fiber and recording sites
498 were tested over auditory cortex, and at each site, we presented broadband noise with half of the
499 trials having a laser delivery simultaneously presented (from 100 ms before, to 100 ms after sound
500 onset/offset; **Fig. 3B-C**). Light delivery affected neural responses in a variety of ways, including
501 suppressing responses to sound, suppressing baseline spontaneous firing and, in some cases, driving
502 firing (**Fig. 3D**). While these patterns were most evident when examining firing in the time window
503 around sound presentation (**Fig. 4A**), the same pattern was also evident in spontaneous activity (**Fig.**
504 **4B**). During spontaneous activity the lower firing rates of units gave less scope to observe
505 modulation and thus the effects of inactivation were weaker.

506 To capture the distinct effects of light delivery on the neural population, we used K-means clustering
507 to classify units into separate groups based on their responses to sounds with and without laser
508 light. Assessing cluster performance with K between 1 and 10 (see Methods) indicated that two
509 clusters captured the majority of variance between units, with the two groups being distinguished by
510 their sensitivity to photostimulation both when considering auditory evoked activity (**Fig. 4C**) and
511 spontaneous activity (**Fig. 4D**).

512 When comparing the effects of laser light on sound evoked firing, Cluster 1 showed a significant
513 decrease with photostimulation (n = 272 units, median change of -1.296 spikes/s, Wilcoxon signed
514 rank test with Bonferroni correction, $p < 0.001$, $Z = -14.3$), whilst Cluster 2 showed a small but
515 significant increase in firing with light delivery (n = 193 units, median change of 0.0667 spikes/s, $p <$
516 0.001 , $Z = 5.09$). In periods of spontaneous activity, Cluster 1 showed a significant decrease in firing
517 with light delivery (median change of -0.4167 spikes/s, Wilcoxon signed rank test with Bonferroni
518 correction, $p < 0.001$, $Z = -8.18$), whilst Cluster 2 showed a similar increase in firing in the
519 spontaneous condition as in the evoked condition (median change of 0.0667 spikes/s, $p < 0.001$, $Z =$
520 4.22).

521 For each unit within a cluster, we also asked if the mean sound-evoked firing rate (windowed
522 between 50 to 150 ms from laser onset, which included 50 ms of baseline activity and the first 50 ms
523 of sound evoked activity) differed between laser presentation and absence (two-tailed sided
524 Wilcoxon signed rank test, $p < 0.05$). The majority of units in Cluster 1 (60.3 %) showed significant
525 decreases in activity with light delivery, while only a minority of units (25.9%) in Cluster 2 were

526 stimulated by light delivery. The pattern of results was similar, regardless of whether activity was
527 recorded from single units or multi-units (**Table 2**).

528 **Spatial and temporal organization of optogenetic inactivation**

529 The extent and speed of inactivation are major considerations when manipulating neural activity
530 during behavior. To understand how far and how fast it was possible to suppress neurons using ChR2
531 expressed via the mDlx promoter, we mapped the effects of laser light with cortical depth and time
532 (**Fig. 5**). In our analysis of depth, we defined the limits of auditory cortex on the basis of sound-
533 evoked responses, of which 95% were observed within 2.62 mm of the top of the probe (**Fig. 5A-B**).
534 Such functional estimates are comparable with the thickness of ferret auditory cortex observed
535 histologically (with correction for tissue shrinkage during fixation, **Fig. 3A**).

536 Across the depth profile of auditory cortex, laser-driven suppression of neural activity was stronger
537 in more superficial units and diminished with distance from the cortical surface (**Fig. 5C**). The effect
538 of depth was evident in the median position of units in clusters 1 and 2 (identified through K-means
539 clustering in the previous section), with light-suppressed units grouped in cluster 1 occurring
540 significantly closer to the cortical surface (rank-sum test, $p < 0.001$).

541 Modeling the laser-related change in single trial spike counts of individual units as a function of
542 distance from the cortical surface confirmed a significant interaction between depth and light
543 delivery (Poisson mixed-model regression with distance and light as fixed effects, ferret, unit and
544 sound duration as random effects, $p < 0.001$). However, the fall-off in suppression captured by the
545 model took place across several millimeters, with 90% of all significantly inactivated units (**Table 2**)
546 being located within 1.598 mm of the cortical surface. This prolonged fall-off over several
547 millimeters contrasts with the rapid attenuation of blue light in tissue over hundreds of micrometers
548 (Li et al., 2019), making it unlikely that light-based artifacts account for the spatial extent of
549 inactivation observed.

550 The temporal profile of inactivation also indicated that the effects we observed were not a trivial
551 result of cortical heating, as light delivery suppressed cortical activity rapidly (**Fig. 5D**).
552 Nonparametric cluster statistics revealed a median latency for significant change in firing at 2.5 ms.
553 Such rapid changes in firing rate show that the mDlx-induced expression of ChR2 in auditory cortex
554 provided a fast method for cortical inactivation, and are unlikely to be driven by changes in
555 temperature of tissue that have been reported over longer time-scales, on the order of hundreds of
556 milliseconds or seconds (Owen et al., 2019).

557 **Optogenetic inactivation primarily affects broad-spiking neurons**

558 Analysis of light-driven suppression of sound driven responses indicated that optogenetic
559 inactivation affected a specific subgroup of neurons; that is units in cluster 1 but not cluster 2,
560 identified through K-means clustering. It is possible that cells within each cluster may be drawn from
561 distinct populations of neurons suppressed by light-driven local network inhibition (cluster 1), and
562 GABAergic interneurons driven by light (cluster 2). Pyramidal neurons and interneurons are often
563 distinguished by their spike waveform as broad and narrow spiking cells respectively (Niell and
564 Stryker, 2008; Moore and Wehr, 2013) and so we asked if the clusters identified from firing rate data
565 might have distinct spike shapes that correspond to these cell types.

566 To compare spike shapes, we measured the trough-to-peak latencies of average spike waveforms
567 from well-isolated single units in cluster 1 (n = 80) and cluster 2 (n = 20) recorded within 1.598 mm
568 from the cortical surface (i.e. the depth range within which 90% of significantly inactivated units
569 were identified). We found that the trough to peak latencies of single units in cluster 1 (i.e. those
570 that were suppressed by the laser) were indeed longer (mean = 0.402 ms) than those in cluster 2
571 (mean = 0.338 ms), indicating a broader waveform (**Fig. 5E**).

572 To determine whether differences in trough-to-peak latency observed between clusters might arise
573 spuriously, we compared the difference we observed in our data with results when randomly
574 shuffling cluster labels (**Fig. 5F**). Permutation testing confirmed that the difference in spike widths
575 between clusters was significant ($p = 0.01$, $n = 1000$ iterations). Thus our results are consistent with
576 the suggestion that neurons suppressed by the laser were primarily broad-spiking
577 excitatory/pyramidal neurons, while the remaining cells were more likely to be narrow-spiking
578 inhibitory interneurons. Note however that because the mDlx promoter is specific only to GABAergic
579 neurons, light is likely to drive multiple subclasses of inhibitory interneurons including, but not
580 restricted to, fast spiking PV neurons.

581 **Auditory cortex is required for vowel discrimination in co-located noise but not clean conditions**

582 We examined the role of primary auditory cortex in behavior using cortical inactivation via cooling in
583 two ferrets (F1311 and F1509) or stimulation of inhibitory interneurons using optogenetics in one
584 ferret (F1706). Ferrets were trained to report the identity of vowel sounds (F1311: /a/ and /i/,
585 F1509, F1706: /u/ and /ε/) of varying sound level in clean conditions (**Fig. 1A**), , and then tested with
586 vowels in additive broadband noise in control conditions and with cooling or laser light delivery.

587 Auditory cortical inactivation impaired vowel discrimination in co-located noise in each animal (**Fig.**
588 **6**). Across SNRs, performance discriminating sounds in noise was worse during cooling than control
589 sessions (change in performance [cooled-control]: F1311 = -11.1%, F1509 = -9.72%) and worse on
590 trials when light was delivered ([Light: On - Off]: F1706 = -12.5%). In contrast, cooling did not impair
591 vowel discrimination in clean conditions in either animal tested (F1311 = +5.39%, F1509 = +1.85%,
592 F1706 not tested with laser light delivery in clean conditions).

593 To assess changes in vowel discrimination with cortical inactivation across ferrets, we compared
594 single trial performance using a mixed-effects logistic regression with ferret as a random effect, and
595 in which background noise (clean vs. noise), experimental treatment (test [cooled or light-on] vs.
596 control [warm or light-off]) and the interaction between treatment and noise were contrasted as
597 fixed effects. We also included whether the subject was rewarded at the center spout and the sound
598 level of vowels as covariates, as well as the interaction between sound level and noise condition.
599 Using the Akaike Information Criterion, this model was selected over other alternatives that either
600 omitted interactions, or included three-way interactions between noise, treatment and sound level.

601 The impairment in vowel discrimination in noise with cortical inactivation was reflected in the fitted
602 model as a significant interaction between noise condition and experimental treatment (**Table 3**, $p =$
603 0.002). There was also a significant main effect of noise ($p < 0.001$) that captured the general
604 impairment of performance caused by degrading sounds. There was no main effect of treatment
605 alone ($p = 0.374$), illustrating that the general ability to perform a two choice task was not affected
606 by cooling/light delivery.

607 **Spatial separation of vowel and noise**

608 In the initial vowel discrimination task, vowels and noise were presented together from two
609 speakers; one on the left and right of the head. We also tested a variant of the task in which vowel
610 and noise were presented either together at a single speaker, or spatially separated from left and
611 right speakers (**Fig. 1B**). In initial behavioral testing, we measured the extent of spatial release from
612 energetic masking in six animals: two ferrets implanted with cooling loops (F1311 and F1509) as well
613 as four additional ferrets that were not used for cortical inactivation (F1201, F1203, F1216 and
614 F1217).

615 Spatial separation of vowel and noise improved the ability of each ferret to discriminate vowel
616 identity compared to co-located vowel and noise (**Fig. 7A**). In terms of percent correct, the benefit of
617 spatial separation was consistent but small for each subject (mean across bootstrap resamples,
618 separated - colocalized; F1311: +1.35%, F1509: +2.85%, F1201: +1.73%, F1203: +2.68%, F1216:
619 1.94%, F1217 = +2.19%). To relate these results to the maximum unmasking possible, we also
620 measured the effect of removing noise entirely by presenting vowels from a single speaker in clean
621 conditions. Removing noise improved performance (mean across bootstrap resamples, clean -
622 colocalized; F1311: 5.78%, F1509: 15.1%, F1201: 26.6%, F1203: 16.7%, F1216: 11.9%, F1217: 20.2%),
623 but no animal performed perfectly in clean conditions (**Fig. 7B**). Thus, although the absolute changes
624 in performance with spatial separation of noise and vowel were small, they could represent a
625 substantial fraction (up to one fifth) of the behavioral benefit observed when removing noise
626 entirely.

627 Spatial separation also improved vowel discrimination in noise during auditory cortical inactivation.
628 In two animals tested with bilateral cooling, performance was better in spatially separated than co-
629 located noise (**Fig. 7C**, separated - colocalized, F1311: +12.7%, F1509: +5.87%). The benefit of spatial
630 separation was larger during cooling than control conditions (F1311: +1.35%, F1509: +2.85%),
631 primarily because cooling impaired vowel discrimination in co-located noise, and the effect of
632 cooling was ameliorated by spatially separating the vowel and noise. The performance benefit of
633 removing noise completely was also evident during cooling (**Fig. 7D**) and more pronounced than in
634 control conditions ([clean - colocalized], cooled vs. control: F1311: 17.5% vs. 5.78%, F1509: 18.1% vs
635 15.1%).

636 To model the effects of spatial separation of vowel and noise on task performance, we fitted a
637 mixed-effects logistic regression to response counts from all animals, with ferret as a random effect
638 and with noise condition (separated vs. co-located), treatment (cooled vs. control), sound level and
639 vowel location (left vs. right) as fixed effects. To account for the possibility that cortical inactivation
640 modulated the effect of spatial separation, we also included an interaction term between treatment
641 and noise condition. Model fitting confirmed the importance of spatial separation ($p = 0.009$) and
642 the effect of cooling on vowel discrimination in noise ($p = 0.011$; **Table 4**), as well as the relationship
643 between task performance and sound level ($p < 0.001$, **Fig. 7E**). There was no significant interaction
644 between cooling and separation, indicating that, at least for the animals tested, cortical inactivation
645 did not affect the performance gained by separating vowel and noise.

646 **A shared role for auditory cortex in sound localization and vowel discrimination in noise**

647 To determine whether the region of auditory cortex that we inactivated was also involved in spatial
648 hearing, we retrained the two ferrets implanted with cooling loops in an approach-to-target sound

649 localization task (**Fig. 1C**). Sound localization was then tested in control conditions and when cooling
650 auditory cortex bilaterally or unilaterally, with cooling of the left or right auditory cortex only.

651 Bilateral cooling impaired sound localization in both ferrets (**Fig. 8A-B**), with performance (percent
652 correct) being significantly lower during cooling than in control testing (change in performance
653 [cooled-control]: F1311 = -14.8%, F1509 = -12.9%).

654 We modeled the effects of bilateral cooling on single trial performance using mixed-effects logistic
655 regression, with treatment [cooled/control] as a fixed effect, and with sound level and center reward
656 as additional covariates in the fixed model. In the random model, we included ferret and speaker
657 location; speaker location was included in the random rather than fixed model to avoid the non-
658 linear dependence of performance on sound location (**Fig. 8C**). The resulting model fit confirmed a
659 significant main effect of cooling, as well as sound level and center reward ($p < 0.001$, **Table 5**).

660 Unilateral cooling impaired localization of sounds in the contralateral hemifield of space to a greater
661 extent than sounds in the ipsilateral hemifield (**Fig. 9A-B**). Cooling left auditory cortex resulted in
662 larger impairments when localizing sounds in the right side of space, compared to the left (mean
663 change in performance across bootstrap iterations, right vs left speakers, F1311: -19.1 vs +0.4%,
664 F1509: -32.5 vs -15.6%). Cooling the right auditory cortex had a less detrimental effect, but again
665 resulted in larger deficits in contralateral localization; here, performance was more strongly
666 impaired when localizing sounds in the left than right side of space for one ferret (change in
667 performance, left vs. right speakers, F1509: -22.9 vs. -6.4%). The same pattern of results was
668 observed in the other ferret, but the difference in performance between speaker locations was
669 much smaller (F1311: -8.3 vs -7.5%). In comparison, the effects of bilateral cooling were similar when
670 localizing sounds in both left and right hemifields (F1311: -14.5 vs. -16.6%, F1509: -15.6% vs. -13.4%).

671 To model performance during unilateral cooling, we used a mixed-effects logistic regression with
672 ferret as a random effect, and fixed effects for cooled hemisphere (left or right auditory cortex),
673 speaker hemifield (left or right side of space) and distance from each speaker to the midline (30°, 60°
674 or 90°). Comparison of nested models demonstrated that interactions between each parameter, up
675 to the level of the three-way interaction significantly improved model fit (analysis of deviance, $p <$
676 0.001) and so we included all interactions between these terms. We also included sound level, the
677 occurrence of a center reward and performance on control trials without cortical cooling (expressed
678 as proportion of trials correct when all other variables were held constant) as covariates.

679 The model captured the larger effect of unilateral cooling on sound localization in the contralateral
680 hemisphere described above as a significant interaction between cooled hemisphere and speaker
681 hemifield ($p = 0.008$, **Table 6**). The interaction between cooled hemisphere, speaker hemifield and
682 angular distance of speaker from the midline ($p < 0.001$) also emphasized how the effects of
683 unilateral cooling were increasingly pronounced at peripheral sound locations (**Fig. 9C**).

684 Discussion

685 Our results, summarized in **Table 7**, demonstrate that both vowel discrimination in noise and sound
686 localization depend on a common region of ferret auditory cortex, and that cortical inactivation via

687 cooling leads to behavioral deficits in both tasks, while leaving intact other forms of hearing such as
688 vowel discrimination in clean conditions.

689 **Selection of cortical region for inactivation**

690 We implanted cooling loops (or optic fibers) over the MEG, specifically targeting the mid-to-low
691 frequency regions of primary auditory cortex (that border the non-primary fields of posterior
692 ectosylvian gyrus; **Fig. 2A**). We targeted this area as it contains neurons that are predominantly
693 tuned to low sound frequencies (Bizley et al., 2005), often vowel responsive and/or spatially tuned
694 (Bizley et al., 2009; Town et al., 2017, 2018) and may play an important role in encoding interaural
695 timing cues supporting sound localization (Wood et al., 2019). It is thus perhaps unsurprising that a
696 region implicated in processing of spatial and non-spatial sound features should contribute to
697 multiple forms of hearing.

698 The extent of inactivation is a critical consideration in any perturbation study (Slonina et al., 2022);
699 the size of cooling loops used here reflected a compromise between the need to inactivate sufficient
700 numbers of neurons to observe behavioral deficits, and avoid unintended spread of cooling to
701 subcortical structures (Coomer et al., 2011). Previous data from our lab has shown that the cooling
702 loops we used induce spatially-restricted heat loss that limits the reduction in spiking activity to the
703 cortical layers surrounding the loop (Wood et al., 2017). In the current study, ferrets could
704 discriminate vowels in clean conditions during bilateral cooling, while in the same sessions, vowel
705 discrimination in noise was impaired. The ability of animals to discriminate vowels in clean
706 conditions demonstrates that the cooling protocol we used did not affect ferrets' general hearing,
707 motor ability or capacity to engage in behavioral tasks.

708 A critical outstanding question is to what extent non-primary regions of auditory cortex beyond MEG
709 contribute to sound localization and vowel discrimination in noise. Earlier cooling studies have used
710 multiple loops to identify distinct contributions of non-primary areas of cat auditory cortex to spatial
711 and non-spatial hearing (Lomber and Malhotra, 2008). If such distinctions also exist in ferrets, then
712 one would predict that inactivation of distinct fields of non-primary auditory cortex may disrupt
713 specific tasks. Testing this will be an important issue for future investigations, which will benefit from
714 the optogenetic techniques that we have confirmed here are effective in rapidly suppressing
715 auditory cortical processing of sounds and disrupting psychoacoustic task performance.

716 **What is auditory cortex doing?**

717 Our results confirm the widely observed role of auditory cortex in sound localization in carnivores
718 (Kavanagh and Kelly, 1987; Smith et al., 2004; Malhotra et al., 2008), while the ability of ferrets to
719 discriminate vowels in clean conditions is consistent with similar behavior in cats with lesions of
720 primary and secondary auditory cortex (Dewson, 1964). Thus, although auditory cortical neurons are
721 strongly modulated by vowel timbre (Bizley et al., 2009), there may be redundant encoding of
722 spectral timbre across multiple cortical fields, or this activity may not be required for the simple two-
723 choice timbre discrimination employed here.

724 A role for auditory cortex in vowel discrimination became evident when we added noise to vowels.
725 An open question from our work is whether the same role for auditory cortex would be observed in
726 clean conditions if vowels were presented closer to ferret's psychophysical thresholds. If so, then our
727 current results might indicate a role for auditory cortex in difficult listening conditions that is

728 consistent with deficits in fine spectrotemporal discriminations following auditory cortical lesions in
729 cats and non-human primates that otherwise have limited effects on easier tasks requiring coarser
730 resolution (Evarts, 1952; Goldberg and Neff, 1961; Diamond et al., 1962; Massopust et al., 1965;
731 Dewson et al., 1969; Heffner and Heffner, 1986). Interpreting lesion studies requires caution, due to
732 the potential for recovery of function; however our results were obtained using reversible methods
733 for which there was minimal opportunity for recovery during cooling, and particularly during rapid
734 optogenetic inactivation.

735 That spatial separation of target vowels and noise maskers benefits vowel discrimination during
736 cortical cooling suggests that subcortical structures can parse the noise and vowel into separate
737 streams. In stark contrast, substantial performance deficits were observed for co-located vowel and
738 noise, emphasizing the importance of auditory cortex in segregating competing co-located sound
739 sources (Mesgarani and Chang, 2012; Bizley and Cohen, 2013). In our results, the spatial separation
740 of target and masker into opposing hemifields may result in the representation of the vowel being
741 comparable to that in clean conditions in the hemisphere contralateral to the vowel, and help
742 animals to compensate for the lack of cortical scene analysis that is critical for resolving co-located
743 sound sources.

744 **Spatial release from energetic masking**

745 The effects of release from energetic masking that we observed were small, relative to the benefit of
746 removing masking entirely. This is not surprising given the limited effectiveness of spatial release
747 from energetic masking relative to release from informational masking that have been widely
748 reported (Brungart, 2001; Jones and Litovsky, 2011). It is likely that the benefit animals received
749 from spatial separation of vowel and masker can be accounted for by the better-ear effect, in which
750 spatial separation elevates the signal-to-noise ratio at one ear (while decreasing the SNR at the
751 opposite ear), and listeners are then able to select information available from the better ear. Such
752 effects may arise by the level of the inferior colliculus (IC) (Lane and Delgutte, 2005), which would, at
753 least in part, explain how ferrets retained a benefit of spatial separation during cortical cooling. One
754 would therefore predict that IC inactivation might result in more effective disruption, particularly
755 when inactivating IC contralateral to the better ear. While cooling such deep-lying structures within
756 the ferret brain would likely affect surrounding brain regions, the potential anatomical specificity of
757 optogenetics makes such experiments feasible in the future.

758 **Auditory decision making**

759 A notable feature of our results, along with the general pattern in the literature on hearing
760 impairments following auditory cortical inactivation, is the preserved ability of animals to perform
761 some sound-based tasks (e.g. vowel discrimination in clean conditions). These findings suggest that
762 substantial redundancy in the auditory system allows alternative pathways to support task
763 performance. The most obvious candidates for this are the ascending pathways from medial
764 geniculate thalamus to secondary auditory cortex that bypass primary fields of the MEG (Bizley et
765 al., 2015).

766 It is also possible that information at earlier stages of the auditory system, in this case about vowel
767 identity (Blackburn and Sachs, 1990; Schebesch et al., 2010), can access brain areas that coordinate
768 behavior and is sufficient for discriminations that have already been learnt (Ponvert and Jaramillo,

769 2019). Our use of reversible inactivation via cooling, which operates on the timescale of minutes /
 770 individual test sessions, suggests that any redundant pathways must come into use rapidly, integrate
 771 seamlessly with normal decision-making processes and occur with minimal need for learning.

772 Understanding how signals in auditory cortex are integrated into behavior is also critical for
 773 determining how deficits in spatial and non-spatial hearing arise, as the impairments observed in
 774 vowel discrimination in noise and sound localization may not have arisen through the same
 775 mechanisms. Cooling suppresses the activity of neurons, and so we might infer that the absence of
 776 spiking degrades cell assemblies that downstream neurons rely on for informed auditory decision
 777 making. Such downstream centers may be located in areas such as the prefrontal cortex (Romanski
 778 et al., 1999; Kaas and Hackett, 2000) or the striatum (Znamenskiy and Zador, 2013). To ascertain the
 779 underlying causes of the deficits we have observed, it will be necessary to combine auditory cortical
 780 inactivation with neural recording in such downstream areas, or to perform targeted manipulations
 781 of specific neural pathways.

782 **A role for areas showing mixed selectivity in perception?**

783 We targeted inactivation to the area of auditory cortex in which neurons have previously shown
 784 mixed selectivity for sound location and vowel identity (Bizley et al., 2009; Walker et al., 2011; Town
 785 et al., 2018). Such mixed selectivity has been observed widely, including across the auditory system
 786 (Cohen et al., 2004; O'Connor et al., 2010; Chambers et al., 2014; Downer et al., 2017; Yi et al., 2019;
 787 Amaro et al., 2021) and may reflect a general process through which neural systems meet the
 788 demands of complex and flexible behaviors (Rigotti et al., 2013; Jazayeri and Afraz, 2017). Our
 789 results show that an area of the brain tuned to multiple sound features makes a contribution to
 790 multiple forms of hearing, and are consistent with broader predictions about the involvement of
 791 mixed selectivity in behavior (Fusi et al., 2016).

792 Mixed selectivity expands the range of dimensions across which groups of neurons can represent
 793 sounds, and so it may be possible to recover detailed information about diverse stimulus sets from
 794 population activity in auditory cortex. However, our ability to observe the use of such information in
 795 animal behavior is still limited, as most behavioral tasks are low-dimensional (i.e. they have only one
 796 or two independent variables along which subjects act)(Gao and Ganguli, 2015). By testing the
 797 effects of cortical inactivation on both spatial and non-spatial hearing in the same subjects, we have
 798 taken some of the first steps towards expanding the study of auditory behavior to higher dimensions
 799 that may be necessary to understand the role of mixed selectivity in everyday hearing.

800 **Figure Captions**

801 **Figure 1. Behavioral task designs. (A)** Vowel discrimination in noise and in clean conditions. Both
 802 vowel and noise were presented from speakers to the left (S_L) and right (S_R) of the head as the animal
 803 held at a center lick port (C). The animal then reported vowel identity by visiting either left (L) or
 804 right (R) response ports. Spectrograms show vowels (e.g. two 250 ms tokens of /u/, separated by 250
 805 ms interval) alone or with additive broadband noise. Vowel identity was always the same for both
 806 tokens, and the animal was required to respond left or right based on that identity (i.e. there was no
 807 requirement to compare the two tokens). **(B)** Vowel discrimination task when vowels were presented

808 from a single speaker in clean conditions, or with noise from the same speaker (colocalized) or the
 809 alternative speaker (spatially separated). Spectrograms and behavioral task arena as shown in A. (C)
 810 Sound localization task in which ferrets reported the location of broadband noise from one of several
 811 speakers in frontal space by approaching a water spout located at each speaker.

812 **Figure 2. Cortical inactivation in behavioral tasks.** (A) Anatomical location of ferret auditory
 813 cortex and positions of cooling loops (blue) implanted in F1311 & F1509 and viral injection in F1706
 814 over the Middle Ectosylvian Gyrus. (Acronyms, A1: Primary auditory cortex, AAF: Anterior
 815 Auditory Field, AEG: Anterior Ectosylvian Gyrus, AVF: Anterior Ventral Field, ADF: Anterior
 816 Dorsal Field, PEG: Posterior Ectosylvian Gyrus, PPF: Posterior Pseudosylvian Field, PSF: Posterior
 817 Suprasylvian Field, VP: Ventral Posterior Auditory Field). (B) Distribution of cortical temperatures
 818 during bilateral cooling (all tasks) and unilateral cooling of left or right auditory cortex (sound
 819 localization only). Scatterplots show temperatures on individual trials measured at the base of each
 820 cooling loop, where contact was made with the cortical surface.

821 **Figure 3. Targeting of optogenetic inactivation and neural responses.** (A) Imaging viral
 822 expression in ferret auditory cortex. Top: Widefield imaging of coronal sections through the
 823 ectosylvian gyrus with the cell bodies labeled with DAPI (blue) and Chr2 labeled with mCherry
 824 (red). Middle / Bottom: Confocal imaging of the injection site showing colocalization of cell bodies
 825 and mCherry expression (outlined). (B) Experimental schematic showing stimulus and light delivery
 826 protocols. (C) Configurations of probe and optic fiber over injection sites within MEG in each ferret
 827 (F1807 and F1801). (D) Peri-stimulus time histogram and raster plots showing responses of four
 828 example units recorded from auditory cortex with and without light delivery in a single laser pulse
 829 (columns 1-3) and a 10 Hz laser pulse (column 4).

830 **Figure 4. Optogenetic inactivation of auditory cortical activity.** (A-B) Scatterplots of firing rate
 831 with and without laser and (C-D) cumulative histograms of change in firing rate with laser light
 832 delivery. Plots show firing rate measured during (A, C) or before (B, D) sound presentation for each
 833 unit, colored by cluster and filled if the change in firing rate between laser conditions was significant
 834 (Wilcoxon signed-rank, $p < 0.05$). Green lines / labels on cumulative histograms mark the proportion
 835 of units (across all clusters) in which laser presentation suppressed spiking activity.

836 **Figure 5. Depth-dependent suppression.** (A) Schematic of probe displaying approximate anatomical
 837 locations in reference to surface calculated by the most superficial depth at which spiking was
 838 observed. (B) The location of auditory evoked units ($n = 72$) as a function of cortical depth from
 839 surface with boxplot showing quartiles with whiskers showing the 95th percentiles. (C) Change in
 840 firing rate with light delivery as a function of cortical depth from surface. Inset shows magnified gray
 841 region with dotted line showing predictions from fitted Poisson mixed-model. (D) Latency of
 842 significant change in firing rate with light delivery as a function of depth. Marker color and shape in
 843 C-D indicates cluster grouping identified via K-means clustering, as in Figure 4. (E) Spike shapes of
 844 well-isolated single-units of cluster 1 (blue, $n = 80$ SUs) and cluster 2 (red, $n = 20$ SUs) recorded
 845 within 1.598 mm of the surface. Data shown as mean \pm standard deviation. (F) Difference in trough to
 846 peak latency of each mean waveform (cluster 1 - cluster 2) for observed data (red dashed line,
 847 difference = 0.0648 ms) or when randomly shuffling clusters labels (histogram, $n = 1000$ iterations)
 848 during permutation testing (97.5th percentile, black line).

849 **Figure 6. Cortical inactivation impairs vowel discrimination in noise, but not clean conditions.**
 850 (A) Performance discriminating vowels in noise ($n = 3$ ferrets) or clean conditions ($n = 2$ ferrets, F1706

851 not tested) during cooling or optogenetic inactivation and in control testing. Scatter plots show
 852 performance across all SNRs or sound levels for each bootstrap ($n = 1000$ iterations), with means shown
 853 as markers. **(B)** Model fit to data (lines) from each ferret discriminating vowels in clean and noise
 854 conditions, with cooling (F1311 and F1509) or optogenetics (F1706, noise only). Scatter plots show
 855 observed data, with marker size showing trial numbers.

856 **Figure 7. Spatial separation improves vowel discrimination in noise.** **(A)** Performance of each ferret
 857 ($n = 6$) in spatially separated or co-located noise in control conditions across SNR. Scatter plots indicate
 858 performance across bootstrap resampling ($n = 1000$ iterations) with mean performance shown by
 859 markers. **(B)** Control performance discriminating vowels in clean conditions (i.e. without noise) vs. co-
 860 located noise. **(C)** Performance of two ferrets during cooling, when discriminating vowels in spatially
 861 separated or co-located noise. **(D)** Performance during cooling when discriminating vowels in clean
 862 conditions vs. co-located noise. **(E)** Mixed-effect model fit (lines) and observed performance (markers)
 863 vs. SNR discriminating vowels in co-located and spatially separated noise.

864 **Figure 8. Effects of bilateral cooling on sound localization.** **(A)** Performance of ferrets ($n=2$) tested
 865 with bilateral cooling during sound localization. Scatter plots show performance on each bootstrap
 866 sample ($n = 1000$) with means indicated by markers. **(B)** Confusion matrices showing behavioral
 867 responses for each speaker and response location in control conditions (unfilled black: F1311 = 1690
 868 trials, F1509 = 1220 trials), and during bilateral cooling (blue: F1311 = 294 trials, F1509 = 115 trials).
 869 **(C)** Performance as a function of sound location predicted by mixed-effects logistic regression (lines)
 870 and observed during behavior (markers) in cooled and control conditions.

871 **Figure 9. Effects of unilateral cooling on sound localization.** **(A)** Performance of ferrets ($n=2$)
 872 localizing sounds in the left and right side of space during unilateral cooling of left or right auditory
 873 cortex, control conditions and bilateral cooling. Scatter plots show performance on each bootstrap
 874 sample ($n = 1000$) with means indicated by markers. **(B)** Bubble plots showing the joint distribution
 875 of behavioral responses for each speaker and response location during unilateral cooling (filled
 876 blue/yellow) and control conditions (unfilled black) for F1311 (top row) and F1509 (bottom row).
 877 Sample sizes in control conditions (F1311 = 1690 trials, F1509 = 1220 trials), and during cooling left
 878 (F1311 = 476 trials, F1509 = 97 trials) or right auditory cortex (F1311 = 536 trials, F1509 = 294
 879 trials). **(C)** Observed behavior (markers) and model prediction (lines) of performance localizing
 880 sounds in left and right sides of space during unilateral cooling.

881

882 Data Availability

883 All code and data associated with the project is available at:
 884 https://github.com/stephentown42/cooling_auditory_cortex

885 Competing Interests

886 No competing interests declared.

887 **Acknowledgements**

888 We would like to thank Dr Tara Etherington for assistance with data collection during cortical cooling
889 and Dr Joseph Sollini for assistance in developing the optogenetic approach. We are also grateful to
890 Dr Erwin Alles for constructing the fiber optic implants used with F1801 and F1807 and Linda Ford
891 for logistical support.

892 Data associated with sound localization of one subject (F1311) has been previously reported in
893 (Wood et al., 2017)

894 This research was funded in whole, or in part, by the Wellcome Trust [a Wellcome Trust / Royal
895 Society Sir Henry Dale Fellowship to JKB, Grant number 098418/Z/12/A], a Royal Society Dorothy
896 Hodgkin Fellowship to JKB, the BBSRC (BB/H016813/1) and the European Research Council
897 (SOUNDSCENE). For the purpose of open access, the author has applied a CC BY public copyright
898 license to any Author Accepted Manuscript version arising from this submission.

899 **References**

- 900 Adriani M, Maeder P, Meuli R, Thiran AB, Frischknecht R, Villemure J-G, Mayer J, Annoni J-M,
901 Bogousslavsky J, Fornari E, Thiran J-P, Clarke S (2003) Sound recognition and localization in
902 man: specialized cortical networks and effects of acute circumscribed lesions. *Exp Brain Res*
903 153:591–604.
- 904 Ahveninen J, Huang S, Nummenmaa A, Belliveau JW, Hung A-Y, Jääskeläinen IP, Rauschecker JP,
905 Rossi S, Tiitinen H, Raji T (2013) Evidence for distinct human auditory cortex regions for
906 sound location versus identity processing. *Nat Commun* 4:1–8.
- 907 Amaro D, Ferreiro DN, Grothe B, Pecka M (2021) Source identity shapes spatial preference in
908 primary auditory cortex during active navigation. *Curr Biol* 31:3875–3883.e5.
- 909 Atencio CA, Sharpee TO, Schreiner CE (2008) Cooperative Nonlinearities in Auditory Cortical
910 Neurons. *Neuron* 58:956–966.
- 911 Bates D, Mächler M, Bolker B, Walker S (2015) Fitting Linear Mixed-Effects Models Using **lme4**. *J Stat*
912 *Softw* 67 Available at: <http://www.jstatsoft.org/v67/i01/> [Accessed July 30, 2021].
- 913 Bizley JK, Bajo VM, Nodal FR, King AJ (2015) Cortico-Cortical Connectivity Within Ferret Auditory
914 Cortex. *J Comp Neurol* 523:2187–2210.
- 915 Bizley JK, Cohen YE (2013) The what, where and how of auditory-object perception. *Nat Rev*
916 *Neurosci* 14:693–707.
- 917 Bizley JK, Nodal FR, Nelken I, King AJ (2005) Functional organization of ferret auditory cortex. *Cereb*
918 *Cortex N Y N* 1991 15:1637–1653.
- 919 Bizley JK, Walker KMM, King AJ, Schnupp JWH (2013a) Spectral timbre perception in ferrets:
920 discrimination of artificial vowels under different listening conditions. *J Acoust Soc Am*
921 133:365–376.
- 922 Bizley JK, Walker KMM, Nodal FR, King AJ, Schnupp JWH (2013b) Auditory cortex represents both
923 pitch judgments and the corresponding acoustic cues. *Curr Biol CB* 23:620–625.
- 924 Bizley JK, Walker KMM, Silverman BW, King AJ, Schnupp JWH (2009) Interdependent encoding of
925 pitch, timbre, and spatial location in auditory cortex. *J Neurosci Off J Soc Neurosci* 29:2064–
926 2075.
- 927 Blackburn CC, Sachs MB (1990) The representations of the steady-state vowel sound /e/ in the
928 discharge patterns of cat anteroventral cochlear nucleus neurons. *J Neurophysiol* 63:1191–

- 929 1212.
- 930 Bowers JS (2017) Grandmother cells and localist representations: a review of current thinking. *Lang*
- 931 *Cogn Neurosci* 32:257–273.
- 932 Brugge JF, Reale RA, Hind JE (1996) The structure of spatial receptive fields of neurons in primary
- 933 auditory cortex of the cat. *J Neurosci Off J Soc Neurosci* 16:4420–4437.
- 934 Brungart DS (2001) Informational and energetic masking effects in the perception of two
- 935 simultaneous talkers. *J Acoust Soc Am* 109:1101–1109.
- 936 Ceballos S, Piwkowska Z, Bourg J, Daret A, Bathellier B (2019) Targeted Cortical Manipulation of
- 937 Auditory Perception. *Neuron* 104:1168–1179.e5.
- 938 Chambers AR, Hancock KE, Sen K, Polley DB (2014) Online Stimulus Optimization Rapidly Reveals
- 939 Multidimensional Selectivity in Auditory Cortical Neurons. *J Neurosci* 34:8963–8975.
- 940 Cohen YE, Russ BE, Gifford GW, Kiringoda R, MacLean KA (2004) Selectivity for the Spatial and
- 941 Nonspatial Attributes of Auditory Stimuli in the Ventrolateral Prefrontal Cortex. *J Neurosci*
- 942 24:11307–11316.
- 943 Coomber B, Edwards D, Jones SJ, Shackleton TM, Goldschmidt J, Wallace MN, Palmer AR (2011)
- 944 Cortical inactivation by cooling in small animals. *Front Syst Neurosci* 5:53.
- 945 David SV, Fritz JB, Shamma SA (2012) Task reward structure shapes rapid receptive field plasticity in
- 946 auditory cortex. *Proc Natl Acad Sci U S A* 109:2144–2149.
- 947 Dewson JH (1964) Speech Sound Discrimination by Cats. *Science* 144:555–556.
- 948 Dewson JH, Pribram KH, Lynch JC (1969) Effects of ablations of temporal cortex upon speech sound
- 949 discrimination in the monkey. *Exp Neurol* 24:579–591.
- 950 Diamond IT, Goldberg JM, Neff WD (1962) Tonal discrimination after ablation of auditory cortex. *J*
- 951 *Neurophysiol* 25:223–235.
- 952 Dimidschstein J et al. (2016) A viral strategy for targeting and manipulating interneurons across
- 953 vertebrate species. *Nat Neurosci* 19:1743–1749.
- 954 Downer JD, Rapone B, Verhein J, O'Connor KN, Sutter ML (2017) Feature-Selective Attention
- 955 Adaptively Shifts Noise Correlations in Primary Auditory Cortex. *J Neurosci Off J Soc Neurosci*
- 956 37:5378–5392.
- 957 Dunn PK, Smyth GK (1996) Randomized Quantile Residuals. *J Comput Graph Stat* 5:236–244.
- 958 Everts EV (1952) Effect of auditory cortex ablation on frequency discrimination in monkey. *J*
- 959 *Neurophysiol* 15:443–448.
- 960 Flesch T, Balaguer J, Dekker R, Nili H, Summerfield C (2018) Comparing continual task learning in
- 961 minds and machines. *Proc Natl Acad Sci U S A* 115:E10313–E10322.
- 962 Földiák P (2009) Neural Coding: Non-Local but Explicit and Conceptual. *Curr Biol* 19:R904–R906.
- 963 Fritz J, Shamma S, Elhilali M, Klein D (2003) Rapid task-related plasticity of spectrotemporal receptive
- 964 fields in primary auditory cortex. *Nat Neurosci* 6:1216–1223.
- 965 Fusi S, Miller EK, Rigotti M (2016) Why neurons mix: high dimensionality for higher cognition. *Curr*
- 966 *Opin Neurobiol* 37:66–74.
- 967 Gao P, Ganguli S (2015) On simplicity and complexity in the brave new world of large-scale
- 968 neuroscience. *Curr Opin Neurobiol* 32:148–155.
- 969 Goldberg JM, Neff WD (1961) Frequency discrimination after bilateral ablation of cortical auditory
- 970 areas. *J Neurophysiol* 24:119–128.
- 971 Harper NS, Schoppe O, Willmore BDB, Cui Z, Schnupp JWH, King AJ (2016) Network Receptive Field
- 972 Modeling Reveals Extensive Integration and Multi-feature Selectivity in Auditory Cortical
- 973 Neurons. *PLOS Comput Biol* 12:e1005113.
- 974 Harrington IA, Heffner RS, Heffner HE (2001) An investigation of sensory deficits underlying the
- 975 aphasia-like behavior of macaques with auditory cortex lesions. *Neuroreport* 12:1217–1221.
- 976 Heffner HE, Heffner RS (1986) Effect of unilateral and bilateral auditory cortex lesions on the
- 977 discrimination of vocalizations by Japanese macaques. *J Neurophysiol* 56:683–701.
- 978 Jasper HH, Shacter DG, Montplaisir J (1970) The effect of local cooling upon spontaneous and evoked
- 979 electrical activity of cerebral cortex. *Can J Physiol Pharmacol* 48:640–652.

- 980 Jazayeri M, Afraz A (2017) Navigating the Neural Space in Search of the Neural Code. *Neuron*
981 93:1003–1014.
- 982 Jones GL, Litovsky RY (2011) A cocktail party model of spatial release from masking by both noise
983 and speech interferers. *J Acoust Soc Am* 130:1463–1474.
- 984 Kaas JH, Hackett TA (2000) Subdivisions of auditory cortex and processing streams in primates. *Proc*
985 *Natl Acad Sci* 97:11793–11799.
- 986 Kavanagh GL, Kelly JB (1987) Contribution of auditory cortex to sound localization by the ferret
987 (*Mustela putorius*). *J Neurophysiol* 57:1746–1766.
- 988 Lane CC, Delgutte B (2005) Neural Correlates and Mechanisms of Spatial Release From Masking:
989 Single-Unit and Population Responses in the Inferior Colliculus. *J Neurophysiol* 94:1180–
990 1198.
- 991 Li N, Chen S, Guo ZV, Chen H, Huo Y, Inagaki HK, Chen G, Davis C, Hansel D, Guo C, Svoboda K (2019)
992 Spatiotemporal constraints on optogenetic inactivation in cortical circuits Huguenard J,
993 Marder E, Petersen CC, eds. *eLife* 8:e48622.
- 994 Lomber SG, Malhotra S (2008) Double dissociation of “what” and “where” processing in auditory
995 cortex. *Nat Neurosci* 11:609–616.
- 996 Lomber SG, Payne BR, Horel JA (1999) The cryoloop: an adaptable reversible cooling deactivation
997 method for behavioral or electrophysiological assessment of neural function. *J Neurosci*
998 *Methods* 86:179–194.
- 999 Malhotra S, Stecker GC, Middlebrooks JC, Lomber SG (2008) Sound Localization Deficits During
1000 Reversible Deactivation of Primary Auditory Cortex and/or the Dorsal Zone. *J Neurophysiol*
1001 99:1628–1642.
- 1002 Maris E, Oostenveld R (2007) Nonparametric statistical testing of EEG- and MEG-data. *J Neurosci*
1003 *Methods* 164:177–190.
- 1004 Massopust LC, Barnes HW, Verdura J (1965) Auditory frequency discrimination in cortically ablated
1005 monkeys. *J Aud Res* 5:85–93.
- 1006 Mesgarani N, Chang EF (2012) Selective cortical representation of attended speaker in multi-talker
1007 speech perception. *Nature* 485:10.1038/nature11020.
- 1008 Moore AK, Wehr M (2013) Parvalbumin-Expressing Inhibitory Interneurons in Auditory Cortex Are
1009 Well-Tuned for Frequency. *J Neurosci* 33:13713–13723.
- 1010 Nakagawa S, Schielzeth H (2013) A general and simple method for obtaining R2 from generalized
1011 linear mixed-effects models. *Methods Ecol Evol* 4:133–142.
- 1012 Nassi JJ, Callaway EM (2009) Parallel Processing Strategies of the Primate Visual System. *Nat Rev*
1013 *Neurosci* 10:360–372.
- 1014 Niell CM, Stryker MP (2008) Highly Selective Receptive Fields in Mouse Visual Cortex. *J Neurosci*
1015 28:7520–7536.
- 1016 O’Connor K, Yin P, Petkov C, Sutter M (2010) Complex Spectral Interactions Encoded by Auditory
1017 Cortical Neurons: Relationship Between Bandwidth and Pattern. *Front Syst Neurosci* 4:145.
- 1018 Ohl FW, Wetzel W, Wagner T, Rech A, Scheich H (1999) Bilateral Ablation of Auditory Cortex in
1019 Mongolian Gerbil Affects Discrimination of Frequency Modulated Tones but not of Pure
1020 Tones. *Learn Mem* 6:347–362.
- 1021 Owen SF, Liu MH, Kreitzer AC (2019) Thermal constraints on in vivo optogenetic manipulations. *Nat*
1022 *Neurosci* 22:1061–1065.
- 1023 Ponvert ND, Jaramillo S (2019) Auditory Thalamostriatal and Corticostriatal Pathways Convey
1024 Complementary Information about Sound Features. *J Neurosci* 39:271–280.
- 1025 Rauschecker JP, Scott SK (2009) Maps and streams in the auditory cortex: nonhuman primates
1026 illuminate human speech processing. *Nat Neurosci* 12:718–724.
- 1027 Rigotti M, Barak O, Warden MR, Wang X-J, Daw ND, Miller EK, Fusi S (2013) The importance of mixed
1028 selectivity in complex cognitive tasks. *Nature* 497:585–590.
- 1029 Romanski LM, Tian B, Fritz J, Mishkin M, Goldman-Rakic PS, Rauschecker JP (1999) Dual streams of
1030 auditory afferents target multiple domains in the primate prefrontal cortex. *Nat Neurosci*

- 1031 2:1131–1136.
- 1032 Schebesch G, Lingner A, Firzlaff U, Wiegrebe L, Grothe B (2010) Perception and neural
1033 representation of size-variant human vowels in the Mongolian gerbil (*Meriones*
1034 *unguiculatus*). *Hear Res* 261:1–8.
- 1035 Slonina ZA, Poole KC, Bizley JK (2022) What can we learn from inactivation studies? Lessons from
1036 auditory cortex. *Trends Neurosci* 45:64–77.
- 1037 Smith AL, Parsons CH, Lanyon RG, Bizley JK, Akerman CJ, Baker GE, Dempster AC, Thompson ID, King
1038 AJ (2004) An investigation of the role of auditory cortex in sound localization using
1039 muscimol-releasing Elvax. *Eur J Neurosci* 19:3059–3072.
- 1040 Town SM, Atilgan H, Wood KC, Bizley JK (2015) The role of spectral cues in timbre discrimination by
1041 ferrets and humans. *J Acoust Soc Am* 137:2870–2883.
- 1042 Town SM, Brimijoin WO, Bizley JK (2017) Egocentric and allocentric representations in auditory
1043 cortex. *PLOS Biol* 15:e2001878.
- 1044 Town SM, Wood KC, Bizley JK (2018) Sound identity is represented robustly in auditory cortex during
1045 perceptual constancy. *Nat Commun* 9:1–15.
- 1046 Walker KMM, Bizley JK, King AJ, Schnupp JWH (2011) Multiplexed and robust representations of
1047 sound features in auditory cortex. *J Neurosci Off J Soc Neurosci* 31:14565–14576.
- 1048 Wilson DE, Scholl B, Fitzpatrick D (2018) Differential tuning of excitation and inhibition shapes
1049 direction selectivity in ferret visual cortex. *Nature* 560:97–101.
- 1050 Wood KC, Town SM, Atilgan H, Jones GP, Bizley JK (2017) Acute Inactivation of Primary Auditory
1051 Cortex Causes a Sound Localisation Deficit in Ferrets. *PLOS ONE* 12:e0170264.
- 1052 Wood KC, Town SM, Bizley JK (2019) Neurons in primary auditory cortex represent sound source
1053 location in a cue-invariant manner. *Nat Commun* 10:1–15.
- 1054 Yi HG, Leonard MK, Chang EF (2019) The Encoding of Speech Sounds in the Superior Temporal Gyrus.
1055 *Neuron* 102:1096–1110.
- 1056 Zhang J, Nakamoto KT, Kitzes LM (2004) Binaural Interaction Revisited in the Cat Primary Auditory
1057 Cortex. *J Neurophysiol* 91:101–117.
- 1058 Zhou B, Green DM, Middlebrooks JC (1992) Characterization of external ear impulse responses using
1059 Golay codes. *J Acoust Soc Am* 92:1169–1171.
- 1060 Znamenskiy P, Zador AM (2013) Corticostriatal neurons in auditory cortex drive decisions during
1061 auditory discrimination. *Nature* 497:482–485.
- 1062

Table 1: Metadata for each subject. Vowel discrimination was tested in clean conditions, with co-located (CL) noise, or spatially separated (SS) noise. Cooling loops implanted in F1216 (asterisk) were persistently blocked and could not be used reliably to achieve bilateral cooling (1 of 14 attempts). Animals implanted with microelectrodes provided single unit recordings for another study (Town et al., 2018).

Ferret	Implant Type	Vowel Discrimination			Sound Localization
		Clean	CL Noise	SS noise	
F1311	Cooling Loops	Yes	Yes	Yes	Yes
F1509		Yes	Yes	Yes	Yes
F1201	Microelectrode Arrays	No	No	Control only	No
F1203		No	No	Control only	No
F1217		No	No	Control only	No
F1216	Cooling Loops*	No	No	Control only	No
F1706	Optic Fibers	No	Yes	No	No
F1801	Anesthetized Recording	No	No	No	No
F1807		No	No	No	No
F1814	Histology	No	No	No	No

Table 2: Proportion of single and multi-units in each cluster that showed a significant change in firing rate with laser light delivery in 50 to 150 ms window after laser onset (Wilcoxon signed rank test, $p < 0.05$).

	Single Unit	Multi-unit	Total
Cluster 1	58 / 103 (56.3%)	106 / 169 (62.7%)	164 / 272 (60.3%)
Cluster 2	16 / 71 (22.5%)	34 / 122 (27.9%)	50 / 193 (25.9%)
Total	74 / 174 (42.5%)	140 / 291 (48.1%)	214 / 465 (46.0%)

Table 3: Model output for mixed-effect model logistic regression (n = 3 ferrets) showing coefficient estimates and standard error for fixed effects. Sample sizes: F1311 = 1914 trials, F1509 = 603 trials, F1706 = 352 trials. Model fit: Marginal $R^2 = 0.076$, Conditional $R^2 = 0.090$.

Fixed Effects	Estimate	Std. Error	Z	P(> z)
Intercept	1.473	0.266	5.538	< 0.001
Treatment	0.151	0.170	0.888	0.374
Noise condition	-0.951	0.263	-3.614	< 0.001
Vowel sound level	0.112	0.325	0.344	0.730
Center Reward	-0.080	0.104	-0.766	0.443
Treatment * Noise	-0.603	0.199	-3.029	0.002
Noise * Level	0.612	0.344	1.78	0.075

Table 4: Coefficients for mixed effects logistic regression model comparing vowel discrimination in co-located or spatially separated noise, with cortical cooling (2 ferrets) and in control conditions (6 ferrets). Trial counts: F1201= 3112 trials, F1203 = 2501 trials, F1216 = 2821 trials, F1217 = 2335 trials, F1311 = 2744 trials, F1509 = 1430 trials. Model fit: marginal $R^2 = 0.022$, conditional $R^2 = 0.029$.

Fixed Effects	Estimate	Std. Error	Z	P(> z)
Intercept	0.173	0.087	1.98	0.047
Noise separation	0.114	0.044	2.62	0.009
Cooling	-0.322	0.126	-2.55	0.011
Vowel sound level	0.740	0.078	9.46	< 0.001
Vowel Location	-0.031	0.042	-0.747	0.455
Cooling * Separation	0.260	0.167	1.55	0.120

Table 5: Model results for comparison of performance localizing sounds during cooling and control conditions (n = 2 ferrets). Sample sizes, control conditions: F1311 = 1690 trials, F1509 = 1220 trials, bilateral cooling: F1311 = 294 trials, F1509 = 115 trials. Model fit: marginal $R^2 = 0.039$, conditional $R^2 = 0.120$.

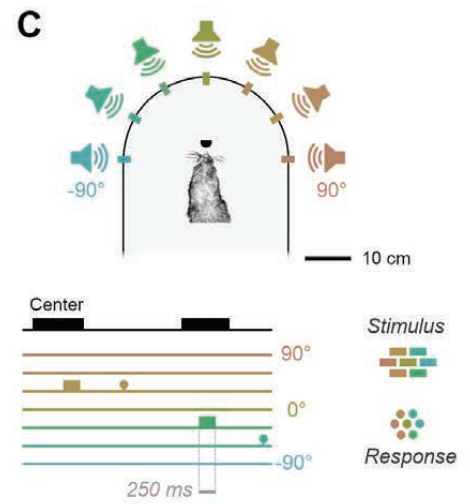
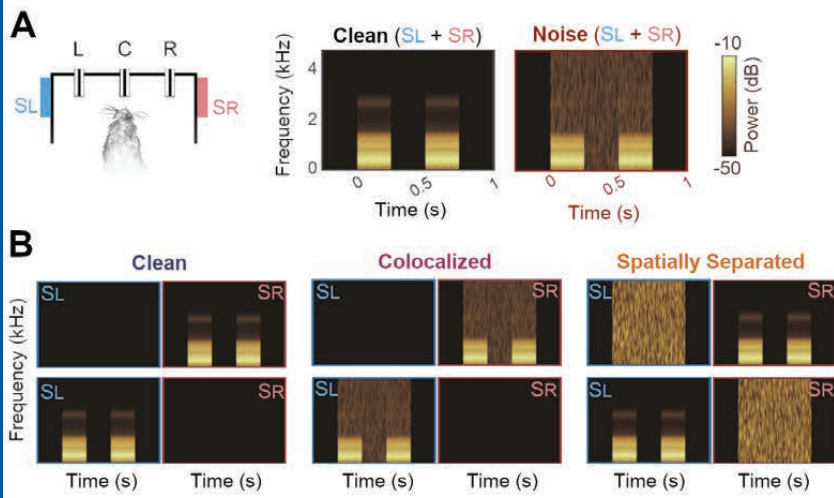
Fixed Effects	Estimate	Std. Error	Z	P(> z)
Intercept	-0.385	0.285	-1.352	0.176
Cooling	0.625	0.111	5.635	< 0.001
Sound level	0.036	0.010	3.668	< 0.001
Center reward	-0.512	0.150	-3.413	< 0.001

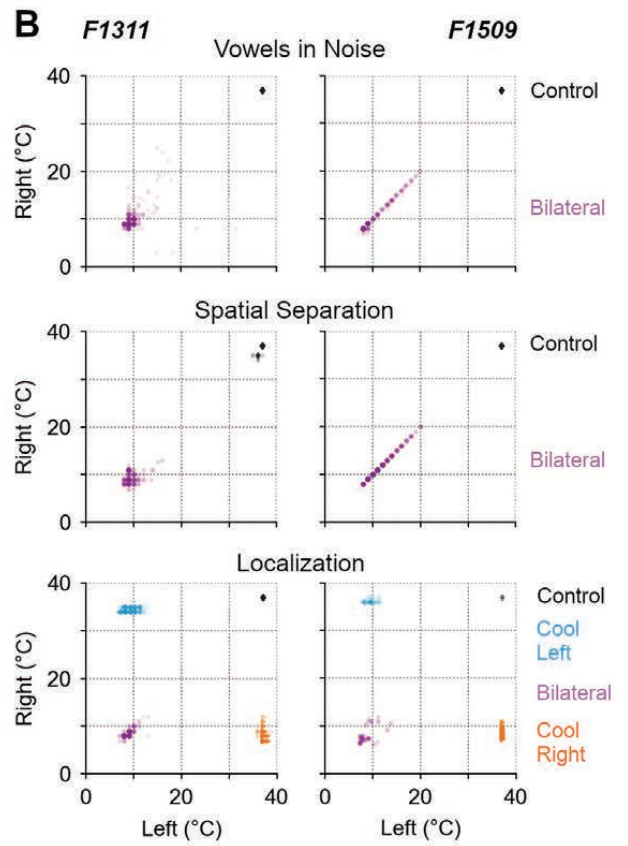
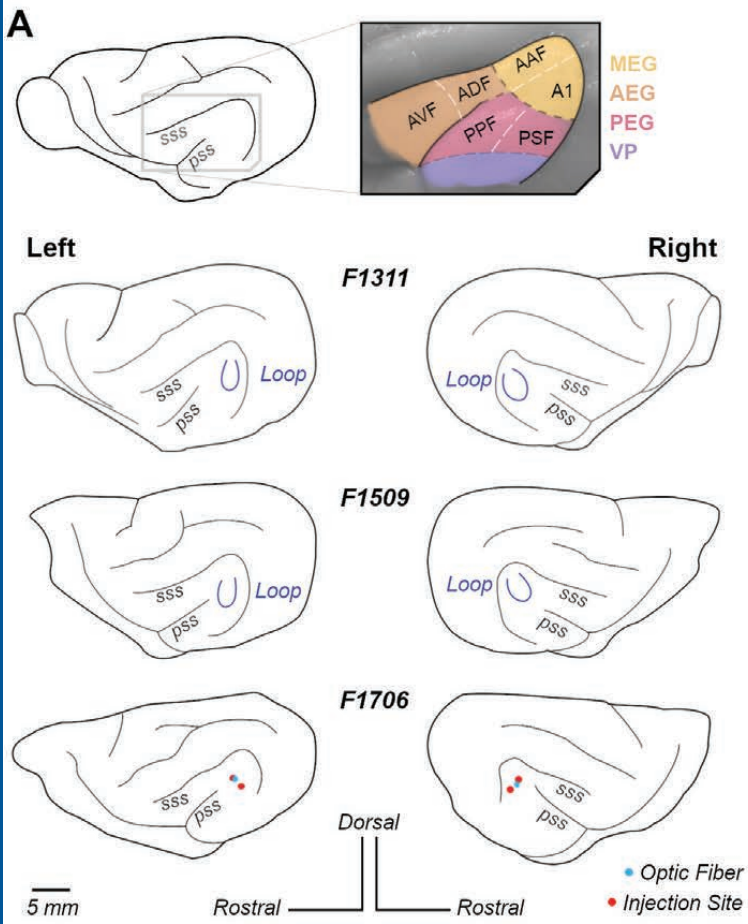
Table 6: Model results for comparison of performance localizing sounds during unilateral cooling of left and right auditory cortex (n = 2 ferrets). Sample sizes during cooling left (F1311 = 476 trials, F1509 = 97 trials) or right auditory cortex (F1311 = 536 trials, F1509 = 294 trials). Model fit: Marginal R² = 0.185, Conditional R² = 0.208.

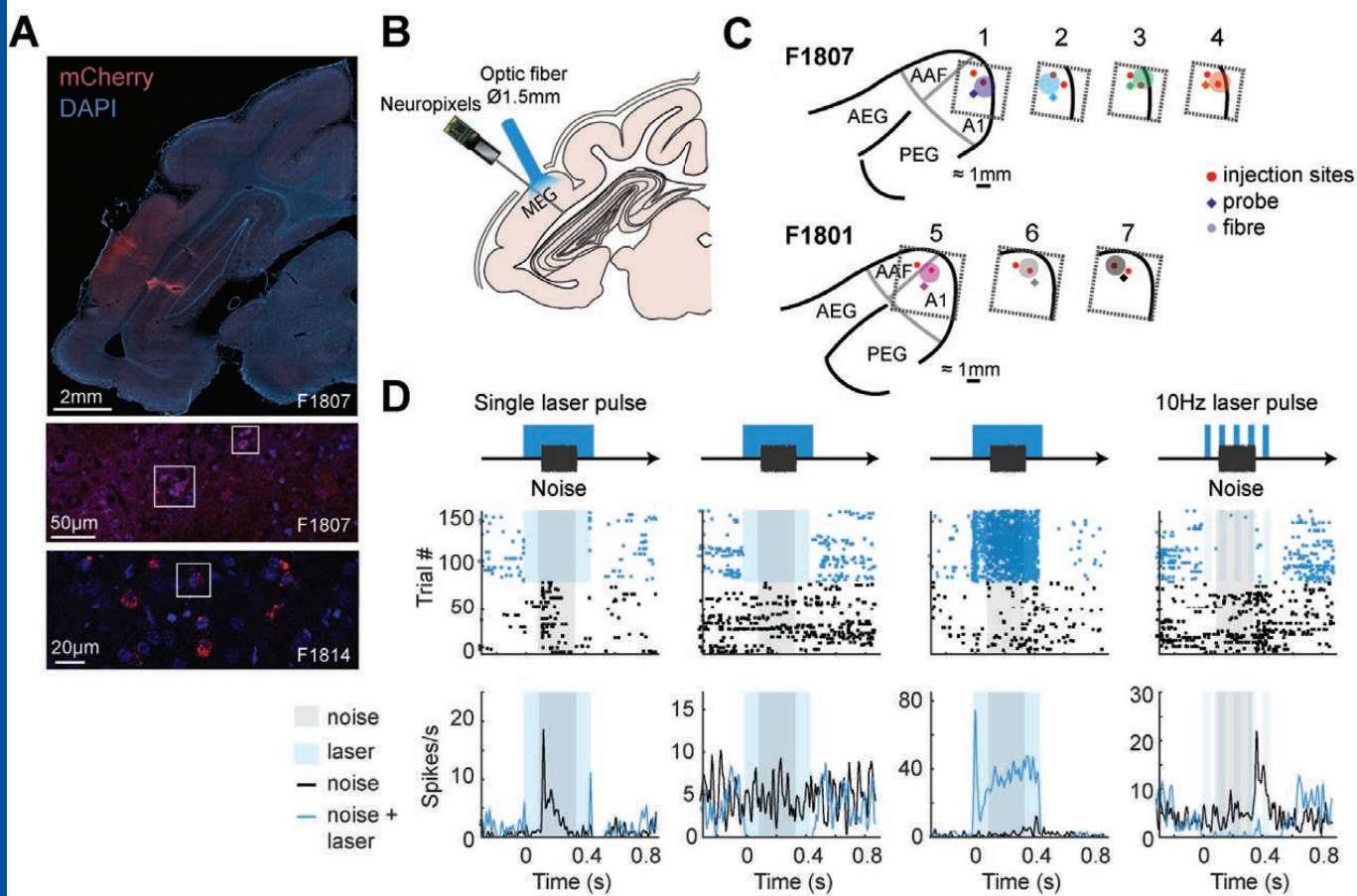
Fixed Effects	Estimate	Std. Error	Z	P(> z)
Intercept	-3.215	0.496	-6.487	< 0.001
Cooled Hemisphere	0.617	0.492	-1.255	0.210
Speaker Hemifield	2.636	0.531	4.968	< 0.001
Angle to midline	2.06	0.390	5.281	< 0.001
Sound level	0.011	0.017	0.637	0.524
Center Reward	-0.082	0.296	-0.276	0.782
Control Performance	2.362	0.419	5.636	< 0.001
Hemisphere * Hemifield	-1.769	0.669	-2.642	0.008
Hemisphere * Angle	-1.138	0.470	-2.419	0.016
Hemifield * Angle	-3.581	0.516	-6.937	< 0.001
Hemifield * Angle * Hemisphere	2.965	0.632	4.694	< 0.001

Table 7: Summary of results during auditory cortical cooling.

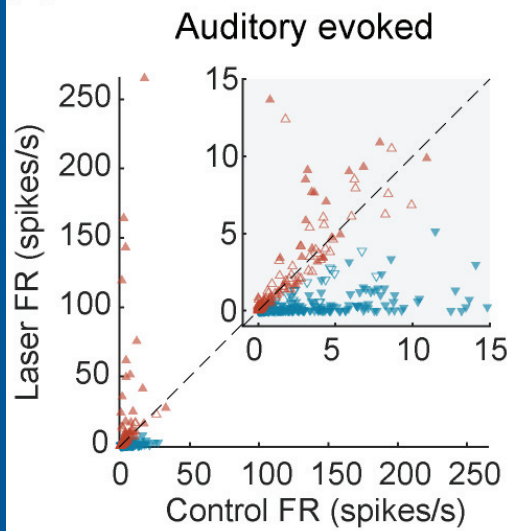
Ferret (method)	Vowel Discrimination			Sound Localization
	Clean	CL Noise	SS noise	
F1311 (cooling)	<i>Present</i>	<i>Impaired</i>	<i>Present</i>	<i>Impaired</i>
F1509 (cooling)	<i>Present</i>	<i>Impaired</i>	<i>Present</i>	<i>Impaired</i>
F1706 (opto.)	<i>Not Tested</i>	<i>Impaired</i>	<i>Not Tested</i>	<i>Not Tested</i>



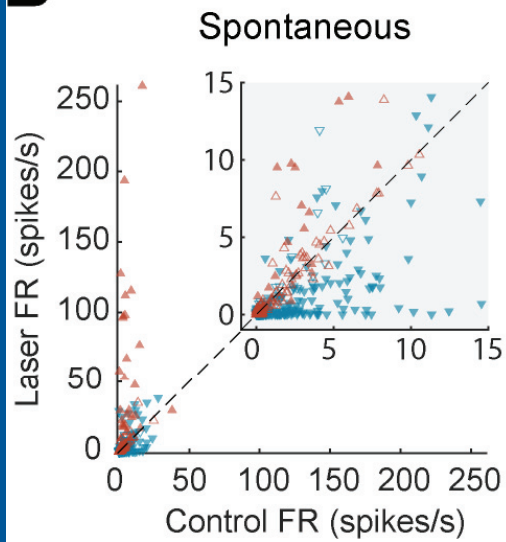




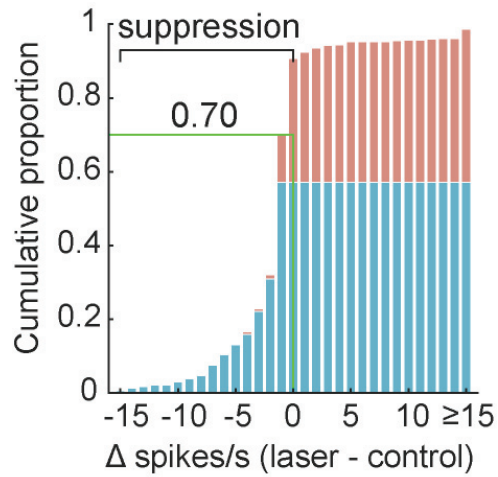
A



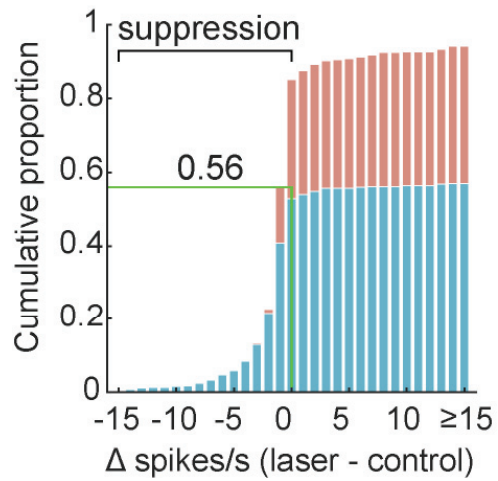
B



C



D



- ▼ cluster 1 ($p < 0.05$)
- ▲ cluster 2 ($p < 0.05$)
- ▼ cluster 1 ($p \geq 0.05$)
- ▲ cluster 2 ($p \geq 0.05$)

